THE DESIGN AND ESTIMATED PERFORMANCE OF A SERIES OF SUPERCAVITATING PROPELLERS

A. J. Tachmindji and W. B. Morgan
David Taylor Model Basin

*   *   *   *   *

This paper outlines the procedure which has been developed for the design of supercavitating propellers and the possible range of application in which such propellers can be used. This design method has been used to predict the performance characteristics of a series of supercavitating propellers and compared with specific experimental results.

*   *   *   *   *

INTRODUCTION

The tendency toward increasing speeds is continuously imposing design limitations on conventional propellers and is providing the impetus for new types of propulsion devices which operate satisfactorily at high speeds. A number of propulsion mechanisms (pumpjets, shrouded propellers) have been investigated with the purpose of delaying the inception of cavitation and its associated effects of erosion and performance breakdown. It becomes apparent, however, that for very high speeds (50 knots and above) suppression of cavitation becomes impossible and it is then necessary to investigate propellers which are designed to operate at low cavitation numbers.

Operation in this speed range results in the back or suction side of the blade sections being completely enclosed within a vapor cavity which originates at the leading edge of the blade and extends beyond the trailing edge. Propellers exhibiting this type of flow configuration are usually known as supercavitating propellers. It should be noted that supercavitating propellers operate completely submerged and are to be distinguished from conventional speedboat propellers which are only partially submerged.

It is the purpose of this paper to outline the procedure which has been developed for the design of supercavitating (SC) propellers and indicate the possible range of application in which such propellers can be used. Certain criteria, which have been derived from experimental information, indicate the operating conditions at which these propellers can be efficiently applied. Furthermore, owing to the somewhat lengthy design calculations and for the purposes of initial estimates it has been deemed desirable to investigate on a theoretical basis the performance characteristics of a series of supercavitating propellers. These results can then be compared with experimental results of specific propellers in order to indicate the accuracy and usefulness of this series.

DESIGN CONSIDERATIONS

Range of Application

The initial decision which has to be made is whether a conventional noncavitating or a supercavitating propeller is the most desirable for specific operating conditions. For conventional propellers it is desirable to have no cavitation on the blades, a condition which is impossible beyond a certain operating speed. In the case of SC propellers the vapor cavity which originates at the leading edge of the blade should collapse beyond the trailing edge in order to prevent erosion of the blades. Experimental results have indicated (1) that in order to have satisfactory supercavitating operation, the cavitation number* of the blade section at 0.7 of the propeller radius, should be less than 0.045; and if the propeller operates at moderate speeds (35 to 50 knots), this requires a high rotational speed. The high rotational speed, however, will result in an inherently low pitch and a correspondingly low propeller efficiency.

Based on the foregoing considerations it has been possible to derive a diagram, shown in Fig. 1, which indicates the areas in which SC propellers become practical. This diagram has H/V_k^2 (which is proportional to the propeller cavitation index) plotted versus the speed coefficient J, where

$$J = \frac{V_a}{nD} \tag{1}$$

and

D = propeller diameter

H = absolute pressure at the shaft centerline minus the cavity pressure (in feet of water)

n = revolutions per unit time

V_a = speed of advance

V_k = speed of advance in knots.

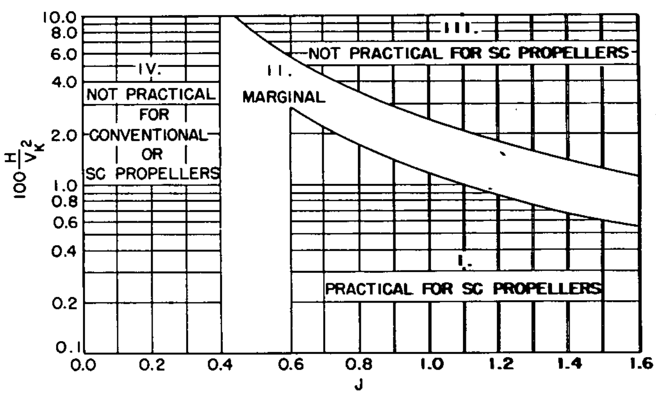

Fig. 1 - Chart of practical application of supercavitating propellers

*See Eq. (20).

In this figure the marginal region (II) above a J of 0.6 is a region of operation in which partial cavitation will probably occur on both conventional and SC propellers. This same region below a J of 0.6 indicates an area in which the propeller efficiency will be low and should be avoided if at all possible.

Study of this diagram will indicate that the speed of advance at which supercavitating propellers become practical is relatively high. Further work has shown, however, that it is possible to decrease the speed of application by artificially increasing the cavity pressure, thus effectively decreasing the section cavitation number. This is achieved by providing an air passage from the back of the blade through which air can be sucked or injected. Such propellers are presently known as ventilated or force-ventilated propellers. For a certain cavitation index, however, it is immaterial whether the cavity is a vapor or an air-cavity and the design considerations which are outlined in this paper are expected to hold equally well in the cases of ventilated propellers. The range of application for these propellers is then only limited by the resulting pressure which can be obtained in the cavity and the operating depth of the propeller.

Choice of Design Parameters

The design of a SC propeller for a given set of design parameters leads to a rather complex investigation and usually results from a compromise between the hydrodynamic considerations, the acceptable stress limits and the practical limitations on propeller diameter.

The first problem considered in connection with the design of the propeller is determining the optimum diameter-rpm relationship. An estimate of this relationship can be obtained from the performance curves which are presented in this paper.

A problem of equal importance with the diameter and rpm is the selection of the number of blades. The choice should be made primarily on the basis of blade stress and vibration. If possible, the number of blades should be chosen so that the blade frequency forces do not cause resonance with any natural frequencies of the ship. As far as stress is concerned (see Appendix A) an individual investigation may be necessary in each case. Decreasing the number of blades will result in an increase in loading, section lift, and hence section thickness. The resultant stress may be either larger or smaller depending on whether the increase in loading or thickness predominate.

For SC propellers the hub diameter may be used, within certain limits, to effectively reduce the blade stress. An increase in hub size will result in an increase in blade loading, but a decrease in bending moment. Since the thickness is a function of blade loading, this increase in loading will result in an increase in thickness and a decrease, up to a certain limit, in stress. Therefore, the changes in both moment and loading will result in a decrease in stress. However, the hub size should not be increased to the point where it materially affects the propeller efficiency.

Other design parameters such as blade chord and section angle of attack are also governed by both the hydrodynamic performance and the structural characteristics of the propeller and must be investigated for a best compromise.

Sections

A critical feature of the design is governed by the choice of sections which are selected to operate in the supercavitating range. The work done by Tulin (2,3) in determining the characteristics of an optimum section within a series of similar shapes, has been the foundation for predicting the characteristics of SC propellers. The results of this work coupled with the experimental investigations of the shapes of these sections (4,5) have provided information extremely useful to the designer.

The work of a number of investigators such as Wu (6), Hug (7), Cohen (8), Johnson (9,10), and others have also been used in the prediction of section characteristics. Their results, however, are essentially similar with Tulin's results within the limits of the basic assumptions. This two-dimensional work has furnished design criteria regarding angle of attack, optimum lift coefficient, and expected drag/lift ratios which are extensively used in the prediction of SC propeller performance. These design considerations are outlined in the parts of this paper describing the design procedure.

DESIGN THEORY

In principle the operation of the SC propeller differs from a noncavitating propeller only in the type of sections used. Hence, the circulation, or lifting-line, theory applies equally well to these propellers.

Two general methods of approach can be considered. The first, developed by Goldstein (11) and extended by Tachmindji (12), deals with the optimum lightly-loaded propeller with a finite number of blades, and the second, developed by Lerbs (13), determines the circulation distribution for moderately-loaded propellers in which the condition of normality is not necessarily assumed. Comparison of the two methods has shown (14) that for the range and load distributions normally encountered in propeller designs, the differences between the two are small. Design calculations in the case of SC propellers have been made using both methods. These calculations have indicated that the circulation distribution factors and the induction factors give essentially the same result.

Based on these two basic approaches, a number of calculations have been made (15-18) which give information directly usable by the designer. From the theory of the optimum propeller, the ideal efficiency (η_i) has been computed (19,20) and can be used in the case of nonoptimum propellers as a first estimate for the hydrodynamic pitch angle (β_i).

The foregoing discussion on propeller theory has been restricted to a blade which has been replaced by a lifting line operating in a nonviscous fluid. In applying this theory to propeller design, the lifting-line considerations have to be expanded to include lifting surface and viscous effects. Ludwieg and Ginzel (21) have examined the curvature of the flow at the midpoint of each section and obtained corrections to the section camber. Lerbs (22) has determined an additional correction in the form of an angle of attack due to change in curvature over the section chord.

The viscous corrections for supercavitating sections and their effect on the ideal efficiency have been derived by Morgan (23).

DESIGN PROCEDURE

Once the propeller diameter, rpm, and hub size have been determined, the propeller can then be calculated. The design can be made either on the basis of thrust or power. Designing on the basis of thrust may be preferable since the variation of thrust between viscous and nonviscous flow is not as great as in the case of power and the speed-resistance relationship is normally more accurately known. The following nondimensional coefficients are computed:

$$\lambda = \frac{V_a}{\pi n D} = \frac{J}{\pi} \tag{2}$$

and

$$C_T = \frac{T}{\frac{\rho}{8} D^2 \pi V_a^2} \tag{3}$$

or

$$C_P = \frac{2\pi Q n}{\frac{\rho}{8} D^2 \pi V_a^3} = \frac{550\ \mathrm{SHP}}{\frac{\rho}{8} D^2 \pi V_a^3} \tag{4}$$

where

D = propeller diameter

n = revolutions per unit time

Q = torque

SHP = shaft horsepower

T = thrust

V_a = $(1 - w_o)V$ = speed of advance of the propeller

V = ship speed

w_o = effective wake fraction

ρ = mass density of fluid.

Since the propeller is calculated on the basis of a nonviscous fluid, the viscous thrust or power coefficient must be modified to their nonviscous values. An approximation for the nonviscous coefficients can be made by assuming that the hydrodynamic pitch angle (β_i) and the drag/lift ratio (ϵ) at 0.7 radius are average values for the propeller, then

$$C_{T_i} \cong \frac{C_T}{1 - 2\epsilon(\lambda_i)_{0.7}} = (1.02 \text{ to } 1.08)C_T \tag{5}$$

$$C_{P_i} \cong \frac{C_P}{1 + \frac{2}{3}\frac{\epsilon}{\lambda_i}} = (0.85 \text{ to } 0.98)C_P \tag{6}$$

where

$$(\lambda_i)_{0.7} = 0.7\ (\tan \beta_i)_{0.7} = \frac{\lambda}{\eta_i}$$

$$\epsilon = 0.1 \text{ as a first estimate.}$$

With Eq. (2) and C_{T_i} or C_{P_i} from Eq. (5) or Eq. (6), the ideal efficiency η_i of an optimum propeller can be obtained from Refs. 19 and 20. Using this value of ideal efficiency the first approximation to the hydrodynamic pitch angle is computed using the relation

$$\tan \beta_i = \frac{\lambda}{x\eta_i} = \frac{\tan \beta}{\eta_i} = \frac{\lambda_i}{x} \tag{7}$$

where

x = nondimensional radius

β = arctan (λ/x) = advance angle

λ_i = λ/η_i (for a free-running optimum propeller).

For an optimum free-running propeller, the ideal efficiency η_i is constant along the blade. If the propeller is not optimum, then η_i varies along the blade and the assumption is made that the ideal efficiency at 0.7 radius is equal to that obtained from the curves.

In order to describe each propeller section, it is necessary to know the radial distribution of hydrodynamic pitch angle β_i, circulation G, coefficient of lift C_L, and thrust coefficient dC_{T_i}/dx or power coefficient dC_{P_i}/dx. These values are derived from the following equations:

$$G = \frac{2x\kappa}{Z} \frac{u_t}{2V_a} \tag{8}$$

$$\frac{C_L \ell}{D} = \frac{2\pi G \cos \beta_i}{\left(\frac{1}{\tan \beta} - \frac{u_t}{2V_a}\right)} \tag{9}$$

$$\frac{dC_{T_i}}{dx} = 4ZG\left(\frac{1}{\tan \beta} - \frac{u_t}{2V_a}\right) \tag{10}$$

$$\frac{dC_{P_i}}{dx} = 4Z\frac{G}{\tan \beta}\left(1 + \frac{u_a}{2V_a}\right) \tag{11}$$

where

$$\frac{u_t}{2V_a} = \left(\frac{\tan \beta_i}{\tan \beta} - 1\right) \frac{\tan \beta_i}{(\tan^2 \beta_i + 1)} = \text{tangential induced velocity}$$

$$\frac{u_a}{2V_a} = \left(\frac{1}{\tan \beta_i}\right)\left(\frac{u_t}{2V_a}\right) = \text{axial induced velocity}$$

ℓ = section chord

Z = number of blades

κ = circulation distribution factor from Ref. 16 or Goldstein factor from Ref. 15.

It should be noted that the integral of dC_{T_i}/dx or dC_{P_i}/dx along the radius should equal the design values of C_{T_i} or C_{P_i}:

$$C_{T_i} = 4Z \int_{x_h}^{1} G \left(\frac{1}{\tan \beta} - \frac{u_t}{2V_a}\right) dx \tag{12}$$

and

$$C_{P_i} = 4Z \int_{x_h}^{1} \frac{G}{\tan \beta} \left(1 + \frac{u_a}{2V_a}\right) dx \tag{13}$$

where x_h is the nondimensional hub radius.

If the propeller is an optimum propeller the difference between C_{T_i} from Eqs. (5) and (12) and between C_{P_i} from Eqs. (6) and (13) will only be within the accuracy with which η_i can be read from the charts. For a nonoptimum propeller the above equations are equally valid, but an iteration procedure is necessary in order to determine the hydrodynamic pitch angle.

The foregoing discussion has been concerned with free-running propellers. For wake-adapted propellers the fact that the wake varies with radius must be considered. Therefore, for the design of these propellers the different coefficients are nondimensionalized on the basis of ship speed instead of speed of advance (14).

Once the desired C_{T_i} or C_{P_i} is obtained, the propeller section shape, section length, and angle of attack can be selected. For SC sections the camberline is the pressure side of the foil and the thickness is applied between the camberline and the free streamline. The maximum ordinate of the pressure side of Tulin's section (2) can be written as follows:

$$(y/\ell)_{max} = 0.5 \sin \theta + (0.1128\, C_L - 0.11817\, \alpha) \cos \theta \tag{14}$$

where

y = face ordinate measured perpendicularly to the nose-tail line

C_L = design lift coefficient

$\theta = (\alpha + \alpha_i)/57.3$ = geometric angles of attack in radians

α = design angle of attack in degrees

α_i = ideal angle of attack in degrees

ℓ = chord length.

For small θ, $\sin \theta \cong \theta$ and $\cos \theta \cong 1$ and Eq. (14) reduces to

$$\begin{aligned}(y/\ell)_{max} &= 0.5\,\theta + 0.1128\, C_L - 0.01182\,\alpha \\ &= 0.1553\, C_L - 0.00426\,\alpha\,. \end{aligned} \tag{15}$$

The distribution of the face ordinates along the chord is given in Table 1.

The thickness of the section, measured normal to the nose-tail line, is given by

Table 1

Distribution of Face Ordinates and Coefficients for Calculating Thickness Along the Chord

x_ℓ	y/y_{max}	F′	N′
0	0	0	0
0.0075	0.01888	-0.001326	0.001254
0.0125	0.03244	-0.002574	0.001870
0.05	0.14189	-0.016816	0.005704
0.10	0.29150	-0.039520	0.010074
0.20	0.56636	-0.078940	0.017349
0.30	0.78458	-0.097600	0.022222
0.40	0.93187	-0.092870	0.024647
0.50	1.0	-0.071780	0.025710
0.60	0.98340	-0.037750	0.025853
0.70	0.87797	0.005940	0.025605
0.80	0.68055	0.056880	0.024660
0.90	0.38860	0.112090	0.023047
0.95	0.20650	0.139620	0.022048
1.0	0	0.166950	0.020937

$$\frac{t}{\ell} = F'C_L + N'\alpha \tag{16}$$

where the coefficients F′ and N′ are also given in Table 1. This equation gives a section slightly thicker than the theoretical cavity shape as shown in Fig. 2. Experimental results (1) have shown that this additional thickness is necessary in order to avoid leading edge vibration and does not affect its performance.

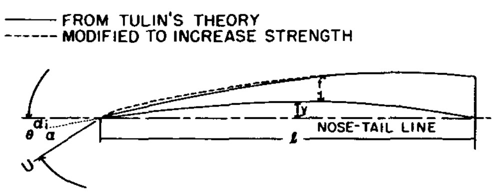

Fig. 2 - Comparison of theoretical and TMB modified thickness distribution of Tulin's SC section

One difficulty encountered in the use of cambered SC sections is pressure face cavitation. If the section is operated at too low an angle of attack for a given camber, face cavitation will occur and poor performance and possibly vibration will result. In addition, it has been shown (1,24) that a certain angle of attack is necessary for the section to have adequate strength. By analyzing a number of experimental results, and noting that theoretically the design angle should be as small as possible in order to obtain minimum drag, the following relationships between design angle of attack α and the coefficient of lift C_L has resulted:

$$\alpha = 36.5\, C_L \quad \text{for} \quad 0 < C_L \leqq 0.0548 \tag{17a}$$

$$\alpha = 2° \quad \text{for} \quad 0.0548 \leqq C_L \leqq 0.2 \tag{17b}$$

$$\alpha = 10\, C_L \quad \text{for} \quad 0.2 \leqq C_L . \tag{17c}$$

It should be noted that Eq. (17a) results in a flat-face section.

Using the above relationships between C_L and α, calculations can be made for the drag/lift ratio ϵ of Tulin's section with part of the lift taken by angle of attack. These calculations have already been made (23) and the results indicate that an optimum lift coefficient for this section is approximately 0.16. This value can then be used in Eq. (9) for estimating the section chord ℓ at 0.7 radius. The blade outline can then be chosen similar to the one given in Table 2.

It is then necessary to determine the stress distribution in the propeller. (A simplified method is given in Appendix I.) In many cases it may be found that the blade outline should be adjusted until acceptable nominal stresses are obtained. This may also be accomplished by an increase in angle of attack towards the root.

Table 2

Radial Distribution of Section Chord

x	$\ell/\ell_{0.7}$
0.20	1.088
0.30	1.088
0.40	1.088
0.50	1.085
0.60	1.062
0.70	1.0
0.80	0.871
0.90	0.655
0.95	0.475
1.00	0

Once the chord, coefficient of lift and angle of attack have been selected the face and thickness can be calculated from Eqs. (15) and (16). The face ordinates, however, must be corrected for the lifting surface effects (14) and are given by

$$(y/\ell)(\text{corrected}) = k_1 k_2 (y/\ell) \tag{18}$$

where k_1 and k_2 are obtained from Fig. 3 and

$$\frac{A_E}{A_O} = \frac{2Z}{\pi} \int_{x_h}^{1} (\ell/D)\, dx = \text{expanded area ratio.}$$

The next step is the calculation of the pitch correction. There are three corrections to be considered; friction correction, effect of finite cavitation number, and correction from lifting surface effect (22). From the data available, it appears that the friction correction is small for these propellers and can therefore be neglected. The effect of finite cavitation number is combined with both the design and the ideal angle of attack into one additional angle of attack (α_1) and is given by

$$\alpha_1 = 57.3\, K_\sigma \theta = 57.3\, K_\sigma (0.0849\, C_L + 0.01512\, \alpha)\ \text{deg} \tag{19}$$

where K_σ is obtained from Fig. (4) and the cavitation number (σ_x) is computed for 0.7 radius, as follows:

$$\sigma_{0.7} = \frac{2gH(\sin^2\beta)_{0.7}}{V_a^2 \cos^2(\beta_i - \beta)_{0.7}} \cong \frac{2gHJ^2}{V_a^2 (J^2 + 4.84)} \tag{20}$$

where g = acceleration of gravity.

The correction for the lifting surface effect results from both free and bound vortices and again occurs as an additional angle of attack α_2 given by

$$\alpha_2 = \alpha_b + (\beta_i - \beta)\left[\frac{2}{1 + \cos^2\beta_i\left(\frac{2}{h} - 1\right)} - 1\right] \tag{21}$$

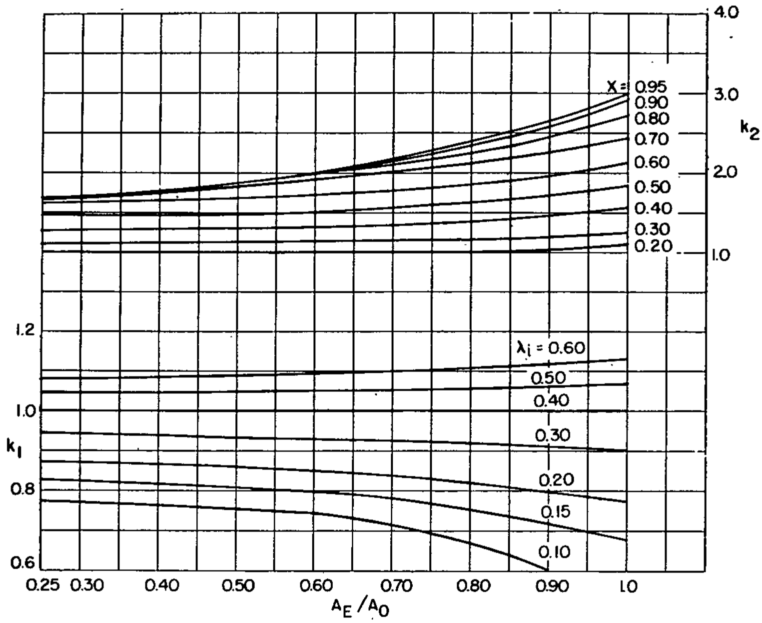

Fig. 3 - Camber correction coefficients

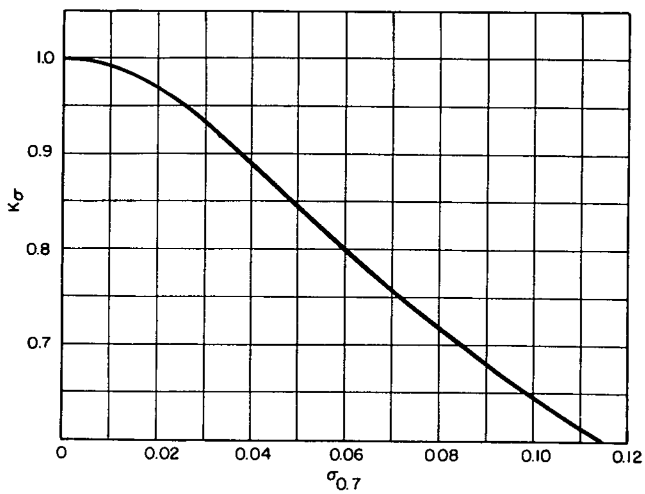

Fig. 4 - Correction to a_1 for finite cavitation number

where h is from Fig. 5 and

$$\alpha_b = 57.3 \left(\frac{\sin \beta_i}{2}\right) \sum_{Z} \left[\frac{\ell}{D} \sin \mu - 0.7 \cos \beta_i \cos \mu \int_{x_h}^{1} \frac{G}{(F/R)^3} dx\right]$$

in which

$$(P/R)^3 = \left[x^2 + \left(\frac{\ell}{D}\right)^2 + 0.49 - 2\left(\frac{\ell}{D} \cos \mu \cos \beta_i + 0.7 \sin \mu\right) x\right]^{3/2}$$

$$\mu = \frac{\pi}{2} + \frac{2\pi}{Z}(m - 1) \quad \text{for} \quad m = 1,2,3 \ldots Z.$$

It should be noted that in Eq. (21) the values of ℓ, β, and β_i are taken at the 0.7 radius and considered constant. This correction is then made at this radius and the same percentage change applied to the other radii.

$$1 + \frac{\Delta P/D}{P/D} = \frac{\tan(\beta_i + \alpha_1 + \alpha_2)_{0.7}}{\tan(\beta_i + \alpha_1)_{0.7}}. \tag{22}$$

The final pitch is then given as

$$P/D = \pi x \left(1 + \frac{\Delta P/D}{P/D}\right) \tan(\beta_i + \alpha_1). \tag{23}$$

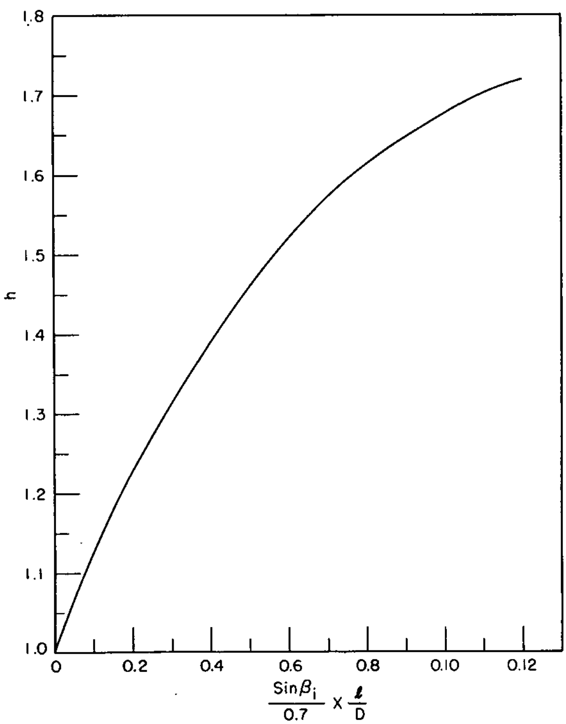

Fig. 5 - Pitch correction coefficient (h) for x = 0.7

With the calculation of the pitch, the design of a propeller is complete except for checking the ratio of C_T to C_{T_i} or the ratio of C_P to C_{P_i} and determining the propeller efficiency. In order to make these calculations it is necessary to know the values of the drag/lift ratio along the radius. These values can be obtained from theoretical (23) or experimental (4) two-dimensional results but must be adjusted for application to propellers (1). Using the foregoing information the following equations for ϵ have been found to give satisfactory results:

$$\epsilon = 0.796 C_L + \frac{0.569}{C_L \left(\log \frac{U\ell}{\nu}\right)^{2.58}} \qquad \text{for } 0 < C_L \leqq 0.0548 \tag{24a}$$

$$\epsilon = (2.14 C_L + 1.13) \left[\frac{(0.4 C_L + 0.0328)^2}{1.5708 C_L} + \frac{0.455}{C_L \left(\log \frac{U\ell}{\nu}\right)^{2.58}}\right] \qquad \text{for } 0.0548 \leq C_L \leq 0.2 \tag{24b}$$

$$\epsilon = (2.14 C_L + 1.13) \left[0.2025 C_L + \frac{0.455}{C_L \left(\log \frac{U\ell}{\nu}\right)^{2.58}}\right] \qquad \text{for } 0.2 \leqq C_L \tag{24c}$$

where

$U = V_a \dfrac{\cos(\beta_i - \beta)}{\sin \beta}$ = section inflow velocity

ν = kinematic viscosity of the fluid.

It is now possible to evaluate the thrust and power coefficient for viscous flow. This check, made at 0.7 radius, gives good results but can be made more accurately by taking into account the drag of each section. The following equations give the viscous thrust and power coefficients as a function of the radius:

$$C_T = \int_{x_h}^{1} (1 - \epsilon \tan \beta_i) \frac{dC_{T_i}}{dx} dx = \int_{x_h}^{1} \frac{\tan \beta}{\tan \beta_i} (1 - \epsilon \tan \beta_i) \frac{dC_{P_i}}{dx} dx \tag{25}$$

and

$$C_P = \int_{x_h}^{1} \left(1 + \frac{\epsilon}{\tan \beta_i}\right) \frac{dC_{P_i}}{dx} dx = \int_{x_h}^{1} \frac{(\tan \beta_i + \epsilon)}{\tan \beta} \frac{dC_{T_i}}{dx} dx . \tag{26}$$

C_T or C_P calculated from the above equations should compare closely with the design values. Also, by using Eq. (25) or Eq. (26) the power or thrust absorbed by the propeller can be calculated and the propeller efficiency η is given by

$$\eta = C_T/C_P. \tag{27}$$

SC PROPELLER SERIES

Propeller series results are usually determined by testing a number of systematic designs and determining their characteristics. In the case of SC propellers, however, this procedure can become extremely costly and time consuming, since all propellers have to be tested over a range of cavitation numbers as well as speed coefficients. With the availability of high-speed computers such characteristics can now be predicted by means of theoretical computations, thus substantially reducing the necessary effort required. The strength or weakness of such a method is of course dependent on the propeller theory on which it is based and the accuracy of its predictions. Calculations of this character should, therefore, be confirmed by means of experimental results in the case of specific propellers, and only then can their accuracy be completely determined. However, if the absolute value of the results is not exactly correct, such a series does provide a means of rapidly determining the relative performance gain or loss which can be obtained by a variation of parameters. Furthermore, such a theoretical series is not intended to replace the design of individual propellers, but can serve as a guide in determining the design conditions. At the present time, it is contemplated that after such conditions are determined the individual design should still be performed.

This series has been derived (25) by designing thirty propellers to cover a range of λ from 0.1 to 0.5 and C_{T_i} from 0.015 to 4.0 at a cavitation number σ of zero. Each propeller has three blades, an expanded area ratio (A_E/A_O) of 0.5, a nondimensional hub radius of 0.2 and used Tulin's sections with the relationship between C_L and α as given by Eq. (17). The Reynolds number, used in calculating the section friction drag, varied between 9.5×10^6 and 5.7×10^7. The results of the calculations, at $\sigma = 0$, are plotted in Figs. 6 and 7 as the square root of the thrust coefficient and the square root of the power coefficient versus the speed coefficient J for various pitch ratios. On these plots are included contours of efficiency and an optimum efficiency line for a given C_T or C_P.

Once the basic design is completed for zero cavitation number the calculations are extended to include finite cavitation numbers ($\sigma_{0.7}$) of the section at 0.7 radius. These calculations result in a change in pitch and are plotted in Figs. 8 and 9 as a function of $\sqrt{C_T}$, J, and $\sigma_{0.7}$. The final pitch is, then, given by

$$P/D = (P/D)_{\sigma=0} - \Delta(P/D)\,C_\sigma \tag{28}$$

where

$(P/D)_{\sigma=0}$ = pitch ratio from Fig. 6 or 7

$\Delta(P/D)$ = pitch correction coefficient from Fig. 8

C_σ = pitch correction coefficient from Fig. 9

$\sigma_{0.7}$ = cavitation number at 0.7 radius from Eq. (20).

The maximum face ordinate at the 0.7 radius is given in Fig. 10 as a function of $\sqrt{C_T}$ and J. Using this ordinate and the distribution of face ordinates along the chord obtained from Table 1 it is possible to calculate the ordinates of this section. The radial distribution of chord can be obtained from Table 2, where ℓ/D at 0.7 radius is 0.351, and the blade thickness fraction (BTF) for this propeller series can be taken from Fig. 11. Additional information for other radii, similar to that given in Fig. 10, is also given in Ref. 25.

A simplified method for calculating the stress has been derived for this propeller series, and the maximum stress (compressive) in psi at the blade root can be estimated by

$$S_c = \frac{0.65\,\rho C_T V_A^2}{144\,(BTF)^2} \cong 0.009\,\frac{C_T V_A^2}{(BTF)^2}\,. \tag{29}$$

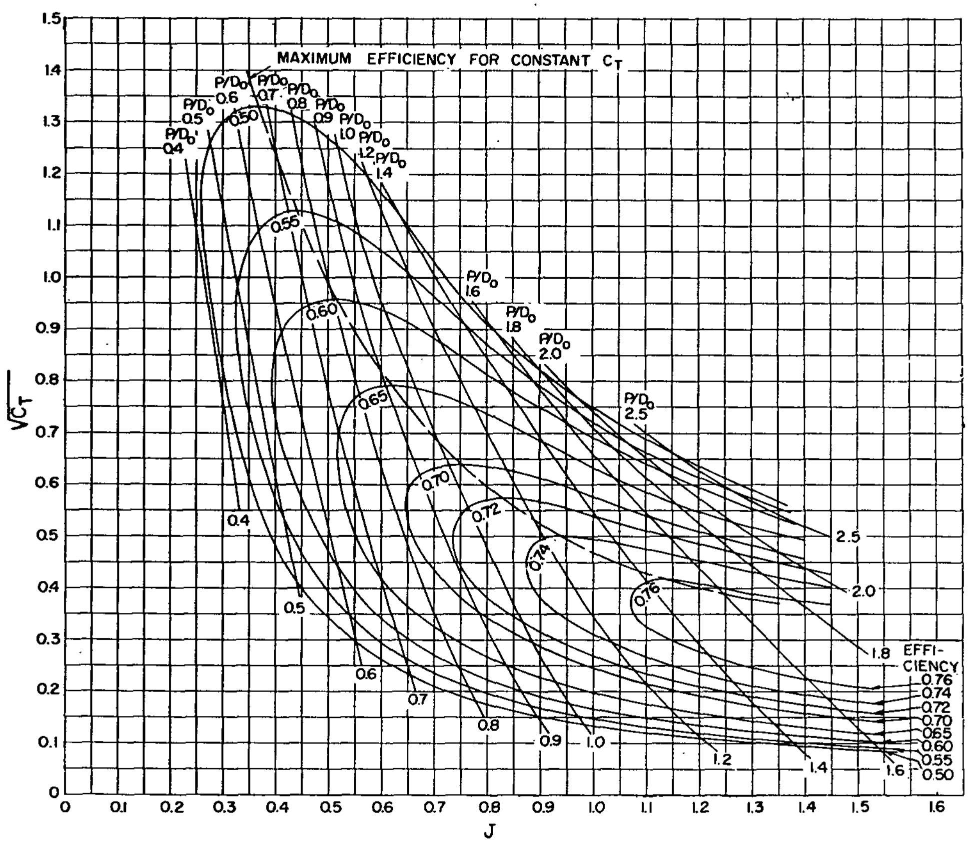

Fig. 6 - C_T - J diagram for TMB SC 3-bladed propeller series

Figures 6 and 7 can also be used to calculate the optimum rpm for a given diameter and the optimum diameter for a given rpm. As an example, the optimum rpm for the following design conditions can be obtained as follows:

$T = 25{,}000$ lbs

$V_a = 101.28$ fps

$D = 3$ ft.

From Eq. (3)

$$C_T = \frac{T}{\frac{\rho}{8}\pi D^2 V_a^2} = 0.35$$

and

$$\sqrt{C_T} = 0.591.$$

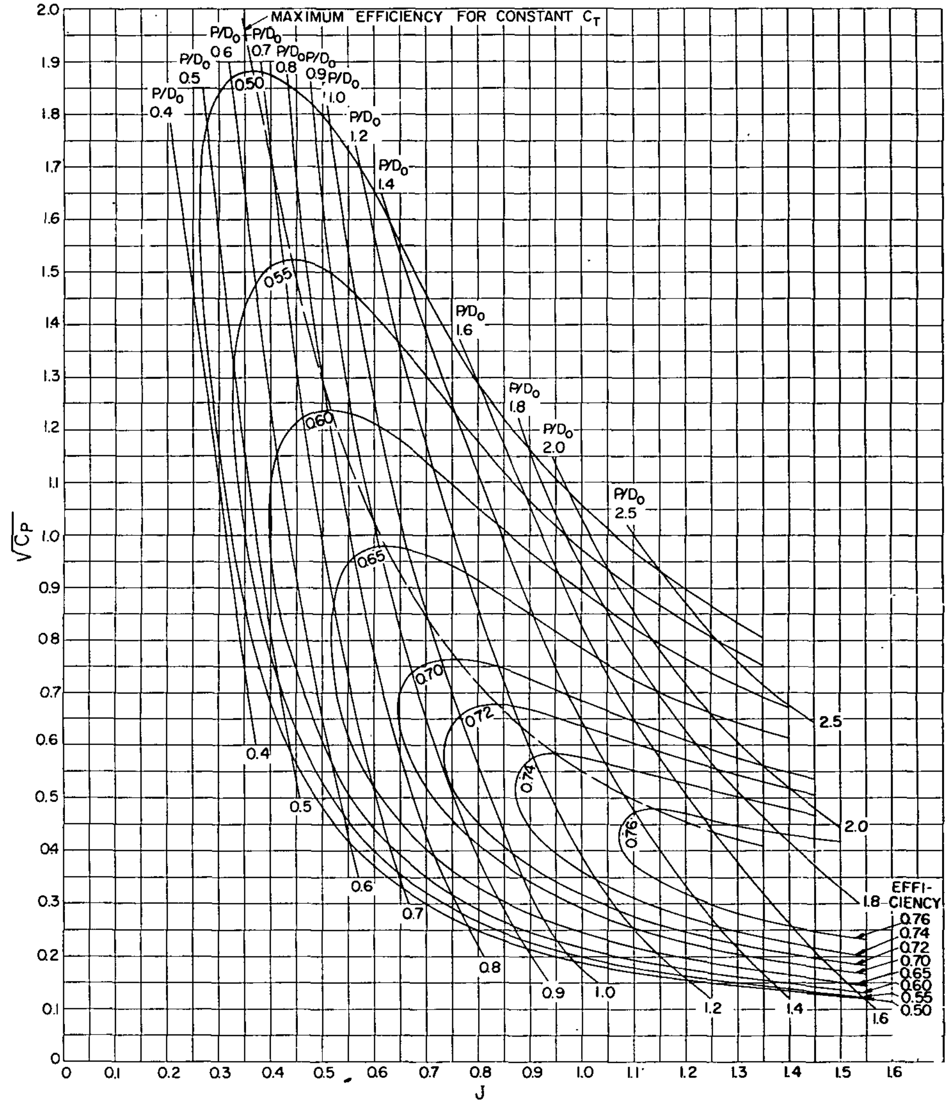

Fig. 7 - C_P - J diagram for TMB SC 3-bladed propeller series

From Fig. 6, the optimum J for this $\sqrt{C_T}$ is 0.815; therefore, the optimum rpm is given by

$$\text{rpm} = \frac{60V_a}{JD} = 2485 \ .$$

The calculation of optimum diameter for a given rpm, speed, thrust, or power can be performed by assuming a diameter and calculating J and $\sqrt{C_T}$ or $\sqrt{C_P}$. A straight line is then drawn through this point and the origin, and the maximum

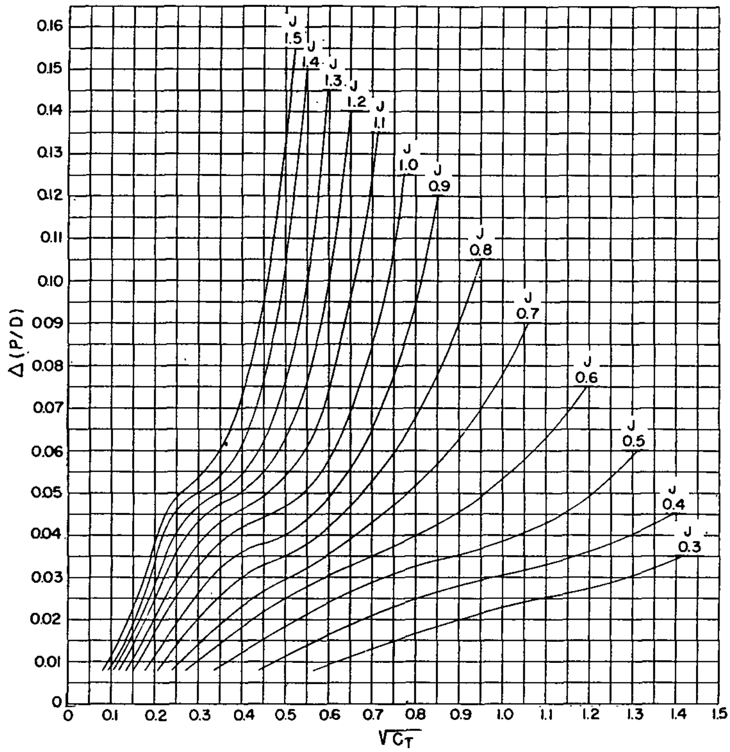

Fig. 8 - Pitch correction coefficient $\Delta(P/D)$ for finite cavitation numbers for TMB 3-bladed SC propeller series

efficiency along this line represents the point at which the diameter is an optimum. An example, for the design conditions

$T = 18{,}000$ lbs

$V_a = 101.28$ fps

$n = 36$ rps

is as follows. Assume that $D = 3$ feet. From Eq. (3)

$$C_T = \frac{T}{\frac{\rho}{8}\pi D^2 V_a^2} = 0.25, \quad \sqrt{C_T} = 0.5, \quad \text{and} \quad J = \frac{V_a}{nD} = 0.94 .$$

This point is then plotted on Fig. 6 and a line is drawn through this point and the origin. The maximum efficiency along this line occurs at a J of 0.9, and the optimum diameter is

$$D = \frac{V_a}{nJ} = 3.13 \text{ feet} .$$

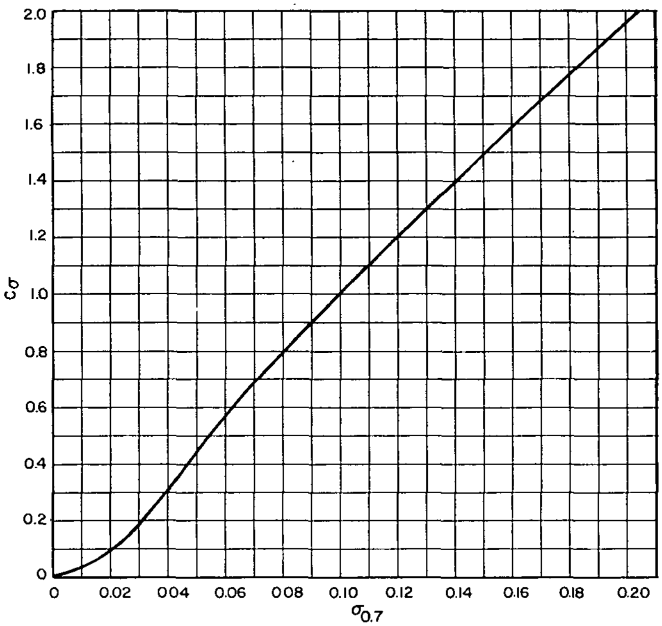

Fig. 9 - Pitch correction coefficient C_σ for finite cavitation number for TMB 3-bladed SC propeller series

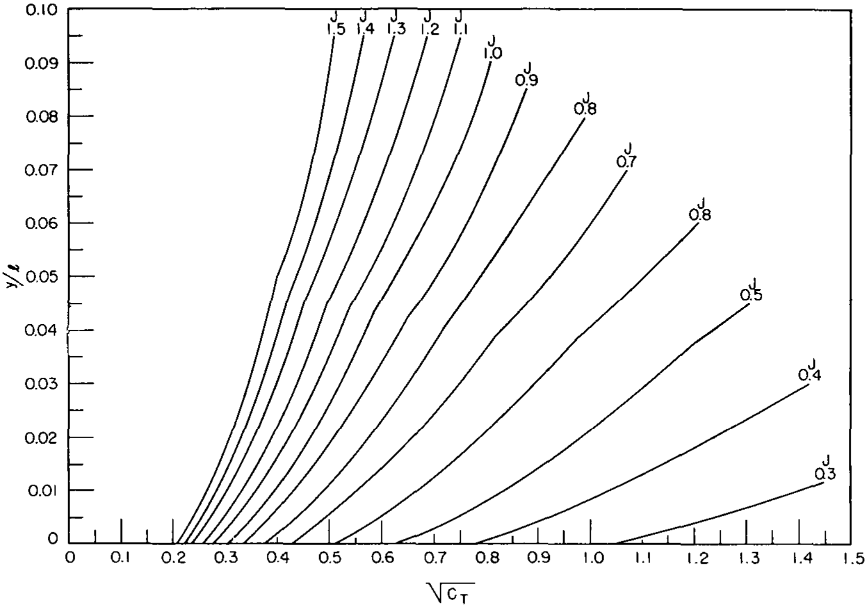

Fig. 10 - Maximum face ordinate at 0.7 radius for TMB 3-bladed SC propeller series

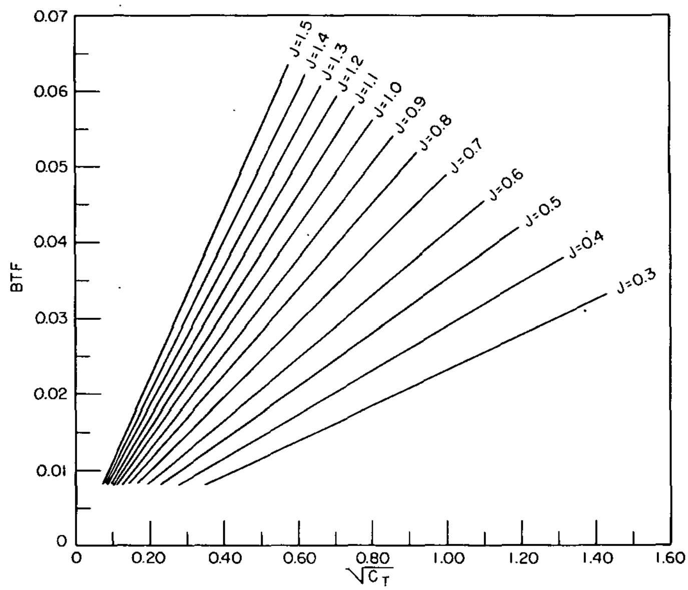

Fig. 11 - Blade thickness fraction for TMB 3-bladed SC propeller series

EXPERIMENTAL RESULTS

A number of tests have been conducted on SC propellers that indicate the adequacy of the design method and practicability of using SC sections on propellers (1). Figure 12 gives the performance characteristics for a 3-bladed propeller designed for 50 knots, 3500 pounds thrust, and 3000 rpm with a diameter of 18 inches. Using nondimensional coefficients these conditions result in a thrust coefficient K_T of 0.140, speed coefficient J of 1.125, and cavitation number $\sigma_{0.7}$ of 0.064. The physical characteristics of this propeller are given in Fig. 13.

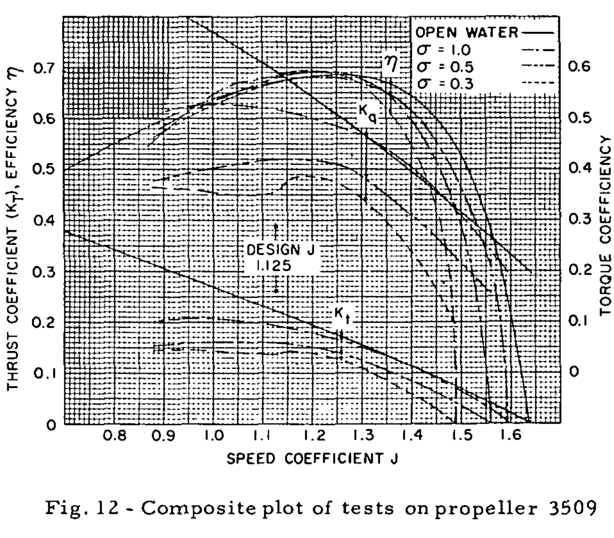

Fig. 12 - Composite plot of tests on propeller 3509

PROP NO	DIA. IN.	PITCH IN.	PITCH RATIO	NUMBER OF BLADES	EXP BLADE AREA	EXP AREA RATIO	MEAN WIDTH RATIO	PROJ AREA	PROJ AREA RATIO	BLADE THICKNESS FRACTION	RAKE ANGLE	ROTATION
3509	18.000	27.601	1.533	3	113.070	.444	.310	84.393	.332	VAR	NONE	RH

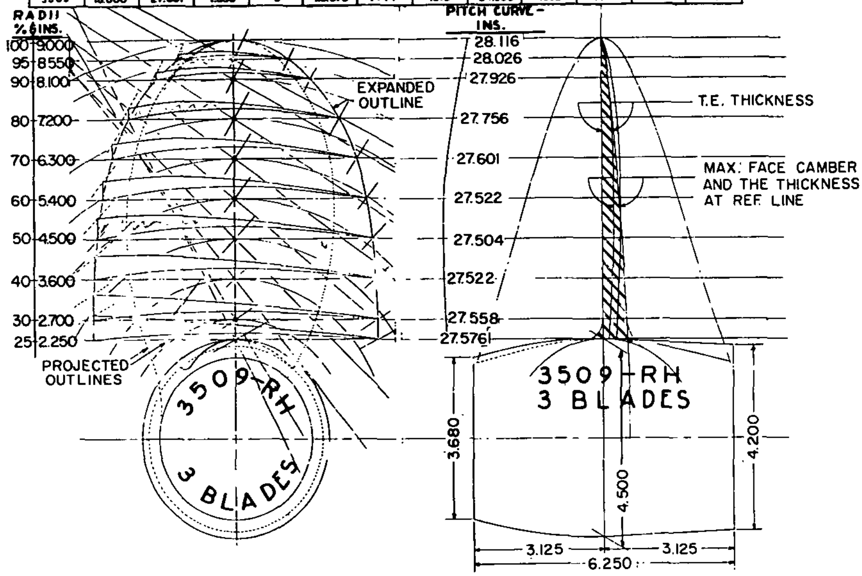

Fig. 13 - Drawing of propeller 3509

From Fig. 12 it can be seen that this propeller gives very close to the design thrust at the design J and also develops an efficiency of approximately 68.5 percent. This propeller has nearly the same characteristics as a propeller obtained from the series previously discussed. From this series for the above design conditions, $C_T = 0.278$ and $J = 1.125$, the propeller would have a P/D of 1.57 and η of 70 percent. It will be noted that these values are in satisfactory agreement with the experimental values.

An interesting characteristic of propellers using SC sections is shown in Fig. 14. This figure is a cross plot from Fig. 12 showing the relationship of thrust coefficient K_t, torque coefficient K_q, and efficiency η to the cavitation number σ at design J. This shows that while cavitation has great effect upon the thrust and torque, it has little effect upon efficiency. The fact that there is a decrease of thrust with decreasing cavitation number is not important as long as the efficiency remains constant and it is possible to meet the design conditions.

Confirmation of the validity of the charts by means of experimental results has also been performed for other propellers. These propellers, however, were 2-bladed and a correction regarding the effect of the number of blades must be introduced. Although such comparisons are not as direct as that performed above, they have indicated agreement between the experimental and predicted results to better than 3 percent.

CONCLUDING REMARKS

The feasibility of supercavitating propellers in the case of high-speed application appears quite promising, particularly where they can be used to the full benefit of

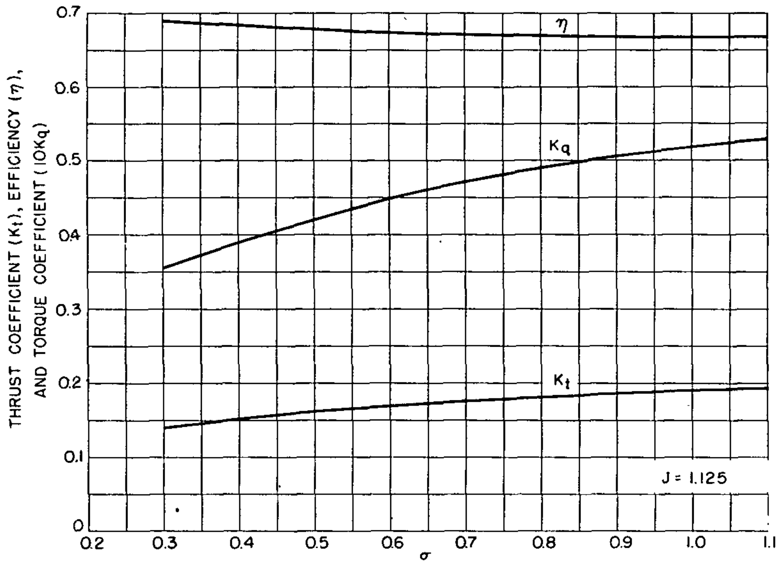

Fig. 14 - Plot of K_t, K_q, and η versus σ for propeller 3509

their hydrodynamic performance. Their range of application may also be extended to lower speeds by the use of ventilated sections.

The design method which has been presented in this paper appears to give results which are verified by experimental confirmation. Improvements in this method, however, can be anticipated as more designs are accomplished and test results become available. The characteristics for the SC propeller series must also be confirmed by means of experimental results for specific propellers and only then can their accuracy be completely determined. It is felt, however, that the series work which has been accomplished to date will provide a method of assessing the effectiveness of the various design parameters. Furthermore, it can certainly be used as an impetus for the design of SC propellers which will exceed these performance characteristics.

ACKNOWLEDGMENTS

The authors wish to thank Captain E. A. Wright, Director of the David Taylor Model Basin, for permission to publish this paper. The assistance of the many members of the Propeller Branch, especially Mr. E. B. Caster, is also greatly appreciated.

NOTATION

A_E/A_O expanded blade area ratio

BTF blade thickness fraction

C_L	section lift coefficient $\left(\dfrac{L}{\frac{\rho}{2} U^2 \ell}\right)$
C_P	power coefficient $\left(\dfrac{2\pi Qn}{\frac{\rho}{8} D^2 \pi V_a^3}\right)$
C_{P_i}	nonviscous power coefficient
C_T	thrust coefficient $\left(\dfrac{T}{\frac{\rho}{8} D^2 V_a^2 \pi}\right)$
C_{T_i}	nonviscous thrust coefficient
C_σ	pitch correction coefficient
D	propeller diameter
F'	coefficient for determining section thickness
G	nondimensional circulation per blade
g	acceleration of gravity
H	absolute pressure at the shaft centerline minus the cavity pressure (in feet of water)
h	pitch correction coefficient
I_{x_0}, I_{y_0}	blade-section-area moments of inertia
J	speed coefficient (V_a/nD)
K_q	torque coefficient ($Q/\rho n^2 D^5$)
K_t	thrust coefficient ($T/\rho n^2 D^4$)
K_σ	correction factor for finite cavitation number
k_1, k_2	camber correction coefficients
ℓ	blade-section chord
M_{Q_b}, M_{T_b}	bending moments on blade section
M_{x_0}, M_{y_0}	bending moments on blade section
N'	coefficient for determining section thickness
n	revolutions per unit time
P/D	pitch ratio
Q	torque
R	maximum propeller radius

r	radius of any propeller blade section
S_c	nominal blade stress
SHP	shaft horsepower
T	thrust
t	section thickness
U	inflow velocity to section $\left[\frac{V_a \cos(\beta_i - \beta)}{\sin \beta}\right]$
u_a	axial component of induced velocity
u_t	tangential component of induced velocity
V	ship speed
V_a	speed of advance
V_k	speed of advance in knots
w_o	effective wake fraction
x	nondimensional radius (r/R)
x_{ℓ}	fractional distance along chord measured from leading edge
y	pressure face ordinate
z	number of blades
α	design angle of attack
α_1	geometric angle of attack corrected for finite cavitation number
α_2	angle of attack from lifting surface effect
α_b	angle of attack for effect of bound vortices
α_i	ideal angle of attack
β	advance angle
β_i	hydrodynamic pitch angle
$\Delta(P/D)$	pitch correction coefficient
ϵ	drag/lift ratio
η	propeller efficiency
η_i	ideal propeller efficiency
θ	geometric angle of attack

κ circulation distribution factor or Goldstein factor

λ advance coefficient

λ_i $x \tan \beta_i$

ν kinematic viscosity of the fluid

ρ density of fluid

σ cavitation number based on propeller speed of advance $(2gH/V_a{}^2)$

σ_x cavitation number based on inflow velocity to the section at x $(2gH/U^2)$

φ pitch angle.

REFERENCES

1. Tachmindji, A.J., Morgan, W.B., Miller, M.L., and Hecker, R., "The Design and Performance of Supercavitating Propellers," David Taylor Model Basin Report C-807, Feb. 1957

2. Tulin, M.P., and Burkart, M.P., "Linearized Theory for Flows about Lifting Foils at Zero Cavitation Number," David Taylor Model Basin Report C-638, Feb. 1955

3. Tulin, M.P., "Supercavitating Flow Past Foils and Struts," Paper No. 16, Symposium on Cavitation in Hydrodynamics, National Physical Laboratory, Teddington, England, 1955

4. Waid, R.L., and Lindberg, Z.M., "Water Tunnel Investigations of a Supercavitating Hydrofoil," California Institute of Technology, Hydrodynamics Report No. 47-8, Apr. 1957

5. Parkin, B.R., "Experiments on Circular Arc and Flat Plate Hydrofoils in Noncavitating and Full Cavity Flows," California Institute of Technology, Hydrodynamics Laboratory Report No. 47-6, Feb. 1956

6. Wu, T.Y., "A Free-Streamline Theory for Two Dimensional Fully Cavitated Hydrofoils," California Institute of Technology, Hydrodynamics Laboratory Report 21-17, July 1955

7. Hug, M., "Theoretical and Experimental Investigations of Forces on Cavitation Hydrofoils," Ph.D. Thesis, University of Iowa, Feb. 1956

8. Cohen, H., and Sutherland, C.D., "Finite Cavity Cascade Flow," Rensselaer Polytechnic Institute, Mathematics Report No. 14, Apr. 1958

9. Johnson, V., "Theoretical Determination of Low-Drag Supercavitating Hydrofoils and Their Two-Dimensional Characteristics at Zero Cavitation Number," NACA RML57 G11A, Sept. 1957

10. Johnson, V., "Theoretical and Experimental Investigation of Arbitrary Aspect Ratio, Supercavitating Hydrofoils Operating near the Free Water Surface," NACA RML57I/6, Dec. 1957

11. Goldstein, S., "On the Vortex Theory of Screw Propellers," Proc. Roy. Soc. (London) 123:440 (1929)

12. Tachmindji, A.J., "The Potential Problem of the Optimum Propeller with Finite Hub," David Taylor Model Basin Report 1051, Aug. 1956, and International Shipbuilding Progress, Nov. 1956

13. Lerbs, H.W., "Moderately Loaded Propellers with a Finite Number of Blades and an Arbitrary Distribution of Circulation," Trans. Soc. Naval Architects Marine Engrs. 60:73-117 (1952)

14. Eckhardt, M.K., and Morgan, W.B., "A Propeller Design Method," Trans. Soc. Naval Architects Marine Engrs. 63:325-374 (1955)

15. Tachmindji, A.J., and Milam, A.B., "The Calculation of Goldstein Factors for Three, Four, Five and Six Bladed Propellers," David Taylor Model Basin Report 1034, Mar. 1956

16. Tachmindji, A.J., and Milam, A.B., "The Calculation of the Circulation Distribution for Propellers with Finite Hub Having Three, Four, Five, and Six Blades," David Taylor Model Basin Report 1141, June 1957, and International Shipbuilding Progress, Oct. 1957

17. Wrench, J.W., Jr., "The Calculation of Propeller Induction Factors, AML Problem 69-54," David Taylor Model Basin Report 1116, Feb. 1957

18. Morgan, W.B., "Propeller Induction Factors," David Taylor Model Basin Report 1183, Nov. 1957

19. Kramer, K.N., "Induzierte Wirkungsgrade von Best-Luftschraben endlicher Blattzahl," Luftfahrt-Forschung, vol. 15, No. 7, NACA Technical Memorandum 884, 1939

20. Shultz, J.W., "The Ideal Efficiency of Optimum Propellers Having Finite Hubs and Finite Numbers of Blades," David Taylor Model Basin Report 1148, July 1957

21. Ludwieg, H., and Ginzel, I., "On The Theory of Screws with Wide Blades," Aerodynamicsche Versuchsanstalt, Report 44/A/108, Goettingen, Germany, 1944

22. Lerbs, H.W., "Propeller Pitch Correction Arising from Lifting Surface Effect," David Taylor Model Basin Report 942, Feb. 1955

23. Morgan, W.B., "Optimum Supercavitating Sections," David Taylor Model Basin Report C-856, Aug. 1957

24. Morgan, W.B., "Centroid and Moment of Inertia of a Supercavitating Section," David Taylor Model Basin Report 1193, Aug. 1957

25. Caster, E.B., "TMB 3-Bladed Supercavitating Propeller Series," David Taylor Model Basin Report 1245, Aug. 1959

26. Morgan, W.B., "An Approximate Method of Obtaining Stress in a Propeller Blade," David Taylor Model Basin Report 919, Oct. 1954

APPENDIX A

STRENGTH ANALYSIS

At the present time there is no theory for which the stress in propellers can be adequately determined. This fact is particularly noted in the design of SC propellers where the sections are inherently thin at the leading edge. Consequently, these propellers are subject to leading edge vibration and fatigue failure. For these reasons it is necessary to use a high-strength material and a large factor of safety. From Ref. 1 it has been concluded that for a material with a 140,000-psi tensile strength the nominal stress of the SC propeller should not be over 30,000 psi.

The nominal stress at any blade section is calculated (26) from the bending moments (M_{x_0} and M_{y_0}), the centroid (x_0 and y_0), and moment of inertia (I_{x_0} and I_{y_0}) by the following equations:

$$\text{Stress at leading edge} = -\frac{y_1 M_{x_0}}{I_{x_0}} - \frac{x_1 M_{y_0}}{I_{y_0}}, \tag{A1}$$

$$\text{Stress in trailing edge on face} = -\frac{y_2 M_{x_0}}{I_{x_0}} - \frac{x_2 M_{y_0}}{I_{y_0}}, \tag{A2}$$

$$\text{Stress on back at maximum back ordinate} = -\frac{y_3 M_{x_0}}{I_{x_0}} - \frac{x_3 M_{y_0}}{I_{y_0}}, \tag{A3}$$

where, as shown in Fig. A1, x_1, x_2, and x_3 and y_1, y_2, and y_3 are used to denote the abscissas and ordinates of the leading edge, face, trailing edge, and point of maximum back ordinate, respectively, measured from the centroid of the section. In these equations a positive stress denotes tension and a negative stress denotes compression.

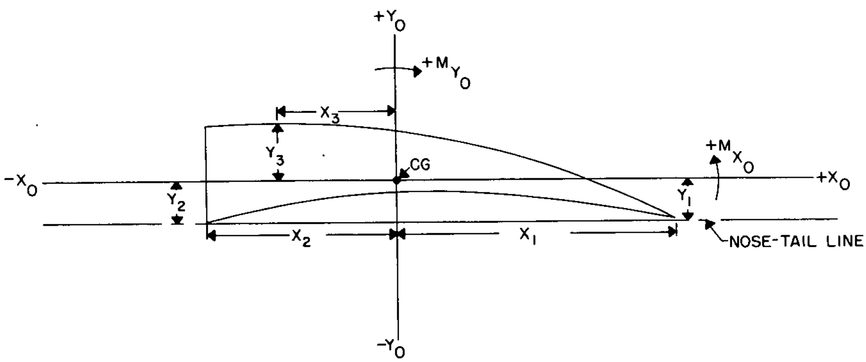

Fig. A1 - Geometric properties of a SC section

In the foregoing equations the bending moments M_{x_0} and M_{y_0} are computed from the thrust and torque moments (M_{T_b} and M_{Q_b}) and the pitch angle φ as follows:

$$M_{x_0} = M_{T_b} \cos \varphi + M_{Q_b} \sin \varphi \cong M_{T_b} \cos \beta_i + M_{Q_b} \sin \beta_i \tag{A4}$$

$$M_{y_0} = M_{T_b} \sin \varphi - M_{Q_b} \cos \varphi \cong M_{T_b} \sin \beta_i - M_{Q_b} \cos \beta_i \tag{A5}$$

where

$$M_{T_b} = \frac{\rho}{2} \frac{R^3 \pi}{Z} V_A^2 \int_{x_0}^{1} (x - x_0)(1 - \epsilon \tan \beta_i) \frac{dC_{T_i}}{dx} dx$$

$$\cong \frac{\rho}{2} \frac{R^3 \pi}{Z} V_A^2 \int_{x_0}^{1} (x - x_0) \frac{dC_{T_i}}{dx} dx$$

$$\cong \frac{\rho}{2} \frac{R^3 \pi}{Z} V_A^2 \int_{x_0}^{1} (x - x_0) \frac{\tan \beta}{\tan \beta_i} \frac{dC_{P_i}}{dx} dx \tag{A6}$$

$$M_{Q_b} = \frac{\rho}{2} \frac{R^3 \pi}{Z} V_A^2 \int_{x_0}^{1} (\tan \beta)(x - x_0)\left(1 + \frac{\epsilon}{\tan \beta_i}\right) \frac{dC_{P_i}}{dx} dx$$

$$\cong \frac{\rho}{2} \frac{R^3 \pi}{Z} V_A^2 \int_{x_0}^{1} (\tan \beta)(x - x_0) \frac{dC_{P_i}}{dx} dx$$

$$\cong \frac{\rho}{2} \frac{R^3 \pi}{Z} V_A^2 \int_{x_0}^{1} (\tan \beta_i)(x - x_0) \frac{dC_{T_i}}{dx} dx \tag{A7}$$

and x_0 is the nondimensional radius of the section being analyzed.

The assumptions that the pitch angle φ in Eqs. (A4) and (A5) is equal to the hydrodynamic pitch angle β_i and that the drag/lift ratio ϵ is zero in Eqs. (A6) and (A7) will have small effect on the bending moments except for heavily loaded propellers.

By comparing a number of calculations, it has been shown (24) that the term xM_{y_0}/I_{y_0} in the stress equation can be neglected for most SC sections. Therefore, only the moment of inertia I_{x_0} and the ordinates need be considered.

Also, if the relationship between C_L and α, as given by Eqs. (17), is assumed, it is possible to considerably simplify the equations for stress. The equations for a flat-face section, (see Eq. 17a) are as follows:

$$\text{Stress at leading edge} \cong -\frac{y_1 M_{x_0}}{I_{x_0}} = \frac{8.2\, M_{x_0}}{\ell^3 C_L^2} \tag{A8}$$

$$\text{Stress at trailing edge on face} \cong -\frac{y_2 M_{x_0}}{I_{x_0}} = \frac{8.2\, M_{x_0}}{\ell^3 C_L^2} \tag{A9}$$

$$\text{Stress at } y_{max} \cong -\frac{y_3 M_{x_0}}{I_{x_0}} = -\frac{10.6\, M_{x_0}}{\ell^3 C_L^2}. \tag{A10}$$

The results for the other relationships given in Eqs. (17) are more complicated and have been combined into nondimensional coefficients $\ell^3 y_1/I_{y_0}$, $\ell^3 y_2/I_{x_0}$, and $\ell^3 y_3/I_{x_0}$ and are plotted in Figs. (A2) and (A3) as a function of C_L and the camber corrections k_1 and k_2. Using those coefficients and neglecting the last term in Eqs. (A1), (A2), and (A3), the calculations of stress for these particular SC sections are considerably simplified.

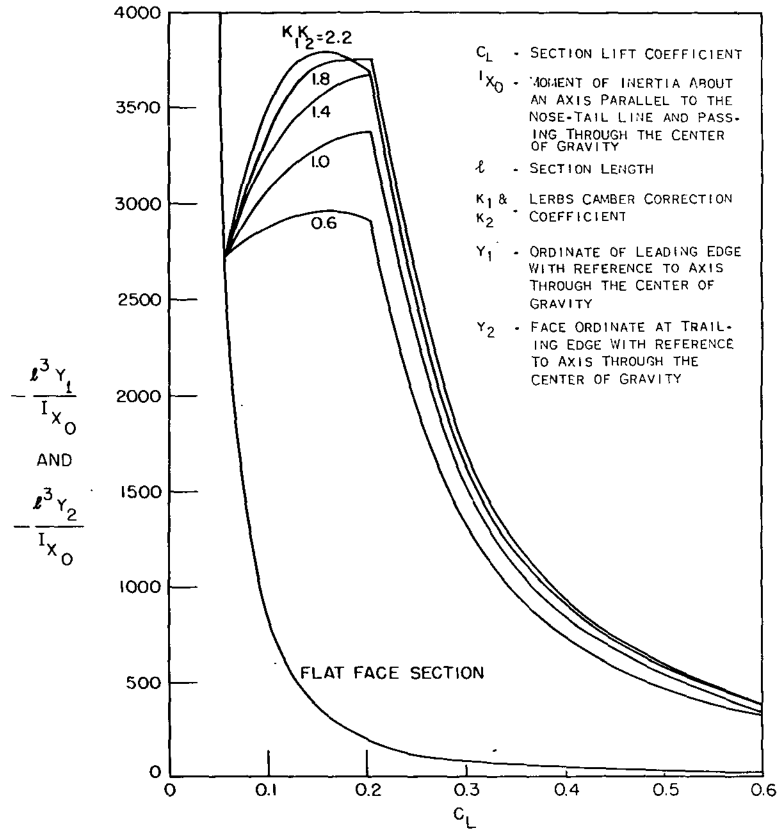

Fig. A2 - Coefficient for determining the stress of the TMB modified SC section

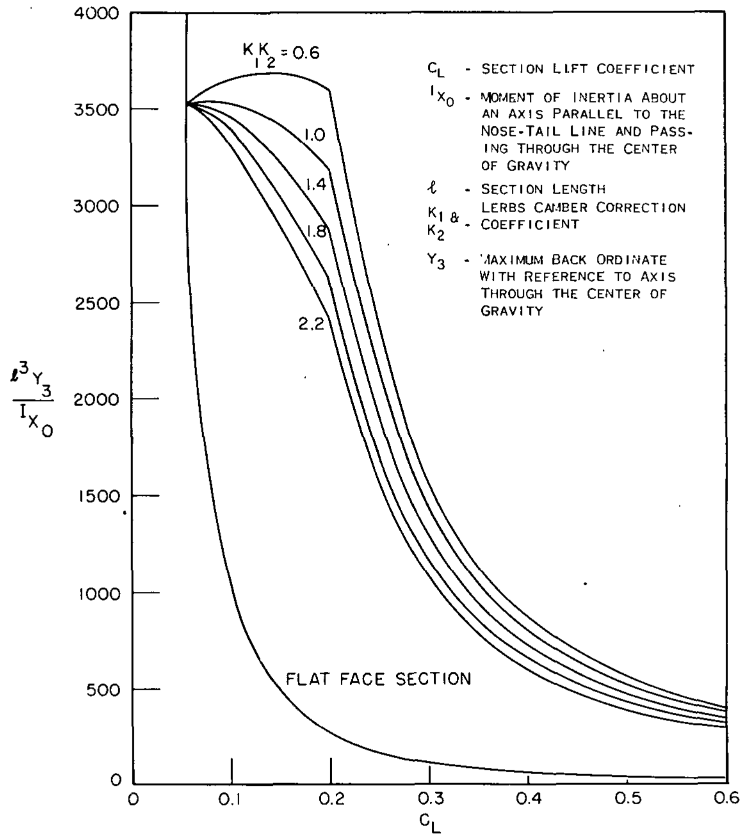

Fig. A3 - Coefficient for determining the stress of the TMB modified SC section

* * * * *

DISCUSSION

H. P. Rader (Vosper, Ltd., England)

The authors of the two papers have given us the benefit of their experience with supercavitating propellers which should be most useful to those interested in high-speed marine propulsion problems.

I would like to take this opportunity to mention a few characteristics of supercavitating propellers which we found during the study of the problem over the last five years.

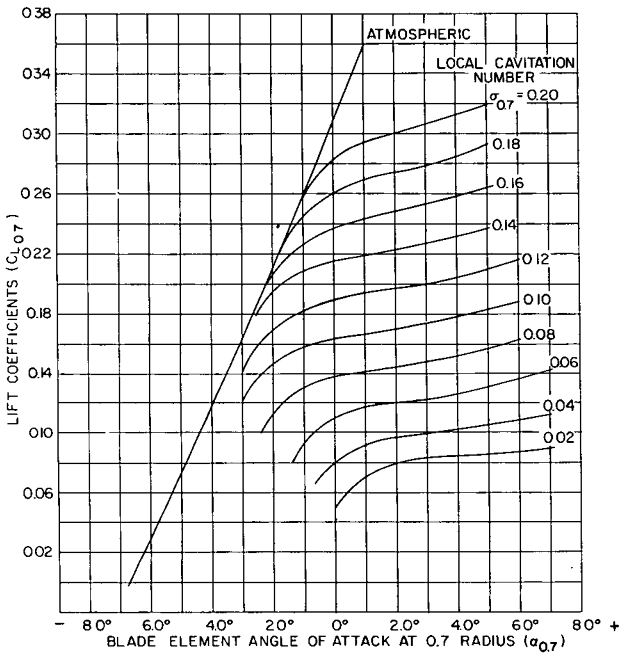

Fig. D1 - Lift coefficients of propeller blade sections at 0.7 radius as function of angle of attack ($\alpha_{0.7}$) with local cavitation number ($\sigma_{0.7}$) as parameter. (Typical values for good, high-speed propellers.)

The advantages of cambered blade sections from the efficiency point of view have been stressed already by Professor Lerbs. I should like to add that flat-faced blade sections are not only less efficient but also inadequate as far as lift production is concerned. Let me explain this. In Fig. D1 the lift coefficients of the equivalent blade section at 0.7 radius for various local cavitation numbers between 0.02 and 0.20 are plotted as function of angle of attack. The curves are obtained from the analysis of the results of cavitation tunnel tests of a good supercavitating propeller with highly cambered blade sections. Please note how small the gradient of these curves is in particular at the low cavitation numbers. For flat-faced blade sections all these curves would be lower and flatter. That means that it is impossible to produce two propellers of the same blade area ratio (B.A.R.), one with cambered and one with flat-faced blade sections, which will produce the same thrust at the same rate of advance even if the pitch of the propeller with the flat-faced sections is increased until it reaches practical limits. The small gradient of the lift-incidence curves is no real drawback. On the contrary, it proves to be a very useful characteristic for high-speed propellers which have to work in a nonuniform velocity field or on a shaft which is inclined relative to the inflow direction. The fluctuations or cyclic variations of the blade element lift components due to incidence changes will be much smaller for a correctly designed supercavitating propeller than for a propeller designed to be free from cavitation.

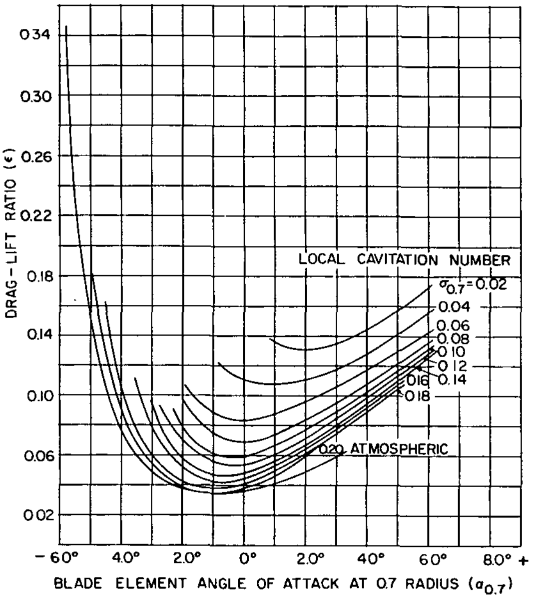

Fig. D2 - Drag-lift ratios of propeller blade sections at 0.7 radius as function of angle of attack ($\alpha_{0.7}$) with local cavitation number ($\sigma_{0.7}$) as parameter. (Typical values for good, high-speed propellers.)

Figure D2 shows the associated values of the drag-lift ratios. The curves for the different local cavitation numbers show more or less pronounced minima which increase with falling cavitation number and move to higher angles of attack. I have to add here that the drag-lift ratios shown in this and the following figures differ from the drag-lift ratios shown by Professor Lerbs. The drag coefficients in the drag-lift ratios shown here include the frictional losses and effects due to finite leading edge thickness, whereas the drag-lift ratios shown by Professor Lerbs allow for pressure drag only. This explains why in Professor Lerbs' graph the drag-lift ratios approach zero as the lift coefficients approach zero, whereas in my graphs the drag-lift ratios have a minimum at a certain angle of attack and approach infinity as the lift coefficients approach zero.

In Fig. D3, values of lift coefficients and drag-lift ratios of the equivalent blade sections at angle of attack $\alpha_{0.7} = 2.5°$, for twelve geometrically similar, supercavitating propellers, are plotted as a function of the local cavitation number. The face camber-chord ratios for blade sections at equal radii are the same, but the thickness-chord ratios of the blade sections at 0.7 radius, for instance, vary from $t/c = 0.034$ for the small blade area ratio propellers to $t/c = 0.016$ for the large blade area ratio propellers. The scatter of the lift coefficient values due to inaccuracies of model manufacture and experimental errors is such that one can draw a mean curve with reasonable fit. This proves the theoretical prediction that for supercavitating conditions the lift coefficient of a blade section depends only on cavitation number, angle of attack, and shape of the face, but not on the basic thickness form of the section. The values of the drag-lift ratios, however, show a definite trend with the thickness-chord ratio of the blade sections. This is due to the fact that it is physically impossible to use infinitely thin leading edges. It appears, however, that the drag-lift ratio for a given lift coefficient and cavitation number is not a function of a representative leading edge thickness but rather it is a function of the edge thickness-to-chord ratio which, of course, is directly proportional to the thickness-chord ratio of the blade section.

Remembering that for propellers of the same diameter which produce the same thrust at the same rate of advance the efficiency depends only on the drag-lift ratio, the possibilities of fully and super cavitating propellers can be assessed best by comparing their drag-lift ratios with those of noncavitating propellers at the same section lift coefficient. Such a comparison is shown graphically in Fig. D4. Values for the supercavitating DTMB propeller number 3509, at the design rate of advance, $J = 1.125$, and the ship cavitation numbers, $\sigma = 0.30$, 0.35 and 0.40, have been added. It appears that in the optimum incidence range the drag-lift ratios of fully cavitating

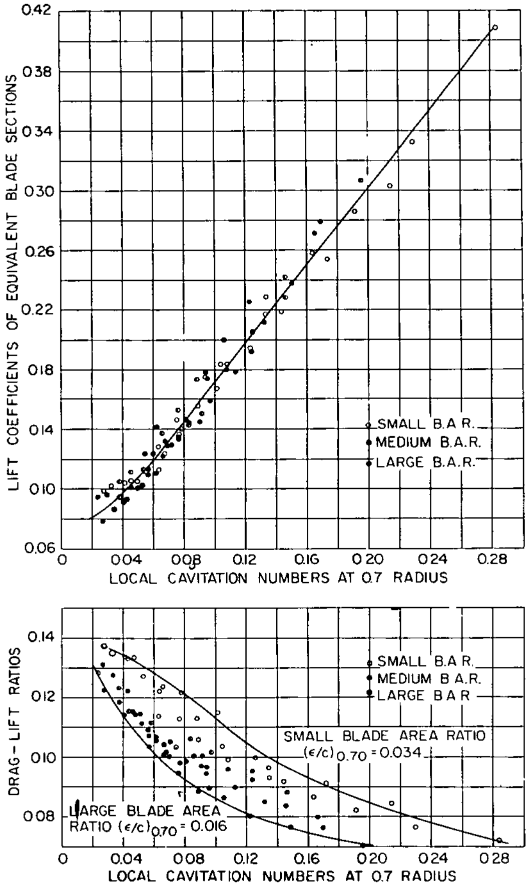

Fig. D3 - Lift coefficients and drag-lift ratios of equivalent blade sections (x = 0.7) at $\alpha_{0.7}$ = 2.5° for twelve geometrically similar supercavitating propellers

propellers are about the same as for noncavitating propellers at the same lift coefficients. This implies, of course, that the lift coefficients for cavitating conditions are lower than for noncavitating conditions at the same angle of incidence or rate of advance. The drag-lift ratios for supercavitating conditions ($\alpha_{0.7}$ = 2.5° and DTMB propeller number 3509) are higher than the absolute minima achieved because the angles of incidence required to obtain sheet cavitation emanating from the leading edge are higher than is consistent with the requirements for minimum drag. This applies, in particular, to supercavitating propellers with narrow blades which require higher face camber ratios and, therefore, higher angles of incidence than supercavitating propellers with medium width or wide blades.

One last point. Mr. Tachmindji quoted as the lower limit for the application of supercavitating propellers a speed of 50 knots. In my opinion this limit is much lower. I would put it at about 35 knots or even lower provided of course the propeller

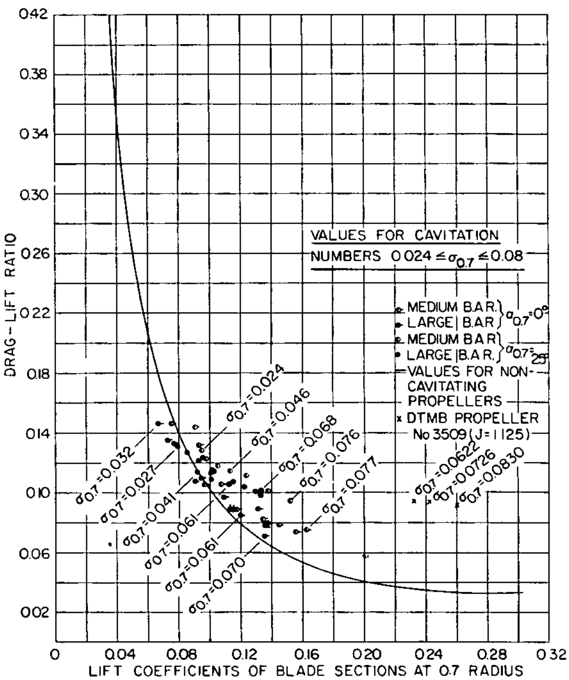

Fig. D4 - Drag-lift ratios of cavitating propellers as function of blade element lift coefficients for 0.7 radius

revolutions are high enough to obtain the low, local cavitation numbers required for supercavitating conditions. Recently we have fitted supercavitating propellers to an 80-ft, passenger launch with a cruising speed of about 35 knots. The performance is as good as it would be with good noncavitating propellers. There are no vibrations and so far the propellers have not shown any signs of cavitation erosion although the propeller shafts are at an angle of about 12 degrees relative to the direction of flow.

M. C. Eames (Naval Research Establishment, Halifax)

It is characteristic of the rapid and efficient manner in which both the theory and application of supercavitating flows have been progressed, that already we have the beginnings of a systematic series of supercavitating propellers. The authors are to be congratulated on this achievement.

I would like to add a word about some of the experimental results. The first open-water tests were conducted on the Canadian R-100 hydrofoil craft (Fig. D5) using DTMB propellers number 3509 and 3604.

This boat displaces 8.5 tons and has a length of 45 feet. The propellers were designed for a speed of advance of 50 knots and were required to develop 3500 pounds thrust at 3000 rpm.

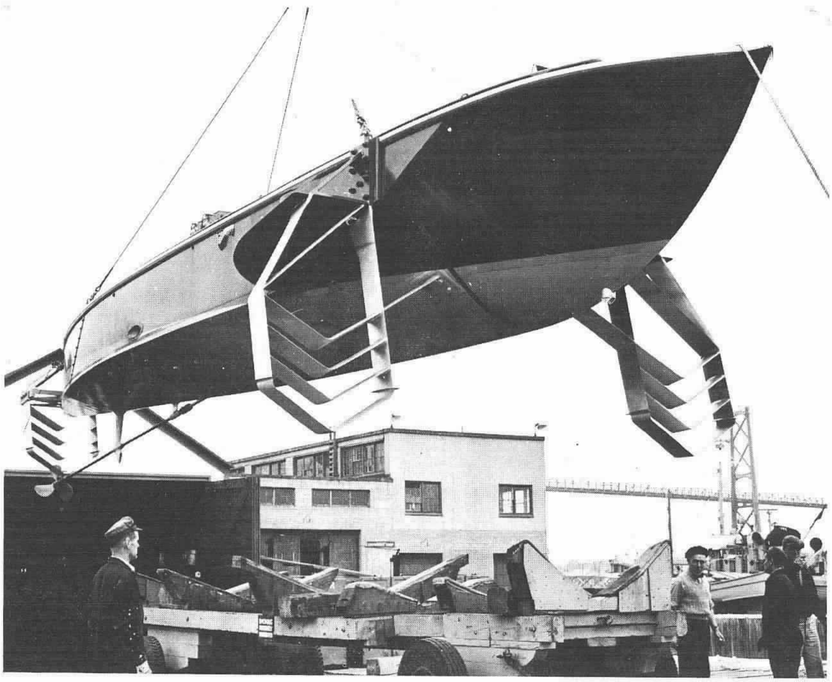

Fig. D5 - Canadian R-100 hydrofoil craft

The first propeller was designed to the theoretical cavity shape, that is to say, without the modified thickness distribution shown in Fig. D6 of the paper. This propeller failed from overstressing the first time a take off was attempted, and performance characteristics could not be obtained. The nature of the failure is shown in Fig. D6. It is believed that a high wake region generated by the stern hydrofoils of the craft was responsible for this failure.

It was anticipated that the strength of this propeller would be marginal, so a second propeller which incorporated the modified thickness distribution was provided. This second propeller is a member of the new DTMB series; Fig. D7 shows it mounted on the craft. The proximity of the lower stern hydrofoil is apparent.

Unfortunately the exact design conditions could not be realized, and it is interesting, in view of Dr. Lerbs' comments, to note that he might have anticipated this. The high-speed lifting foils of the boat use a Walchner section, and it has been found that cavitation occurs on these foils at a lower speed than predicted from Walchner's experimental results. In consequence of this early cavitation, the drag of the craft was significantly higher than predicted and the design thrust of 3500 pounds was demanded at about 40 knots instead of 50 knots.

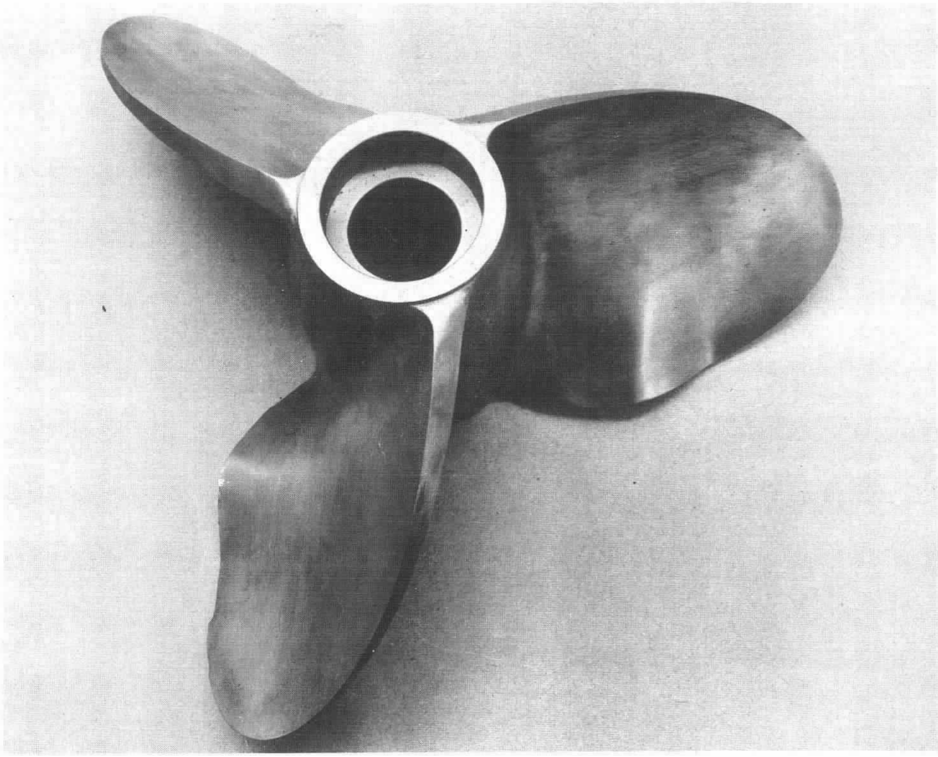

Fig. D6 - Propeller of theoretical cavity shape, without modified thickness, showing wake failure

Despite the fact that the propeller was operating off its design condition, the results were most encouraging. Figure D8 shows the overall propulsive efficiency, defined as thrust horse power (t.h.p.)-to-shaft horse power (s.h.p.) at the engine, plotted on a base of speed in knots. The dotted curve is representative of results obtained with a conventional propeller of N.R.E. design, while the full curve shows the performance of DTMB propeller SC 3604.

Since a hydrofoil craft, with its inherently high speed of advance, is a natural application for the supercavitating propeller, these results are of interest apart from their verification of the propeller design itself. They point out the difficulty which must be faced under take-off conditions where a high drag exists in a speed range of low efficiency for the supercavitating propeller. During these particular trials, take-off was only just achieved.

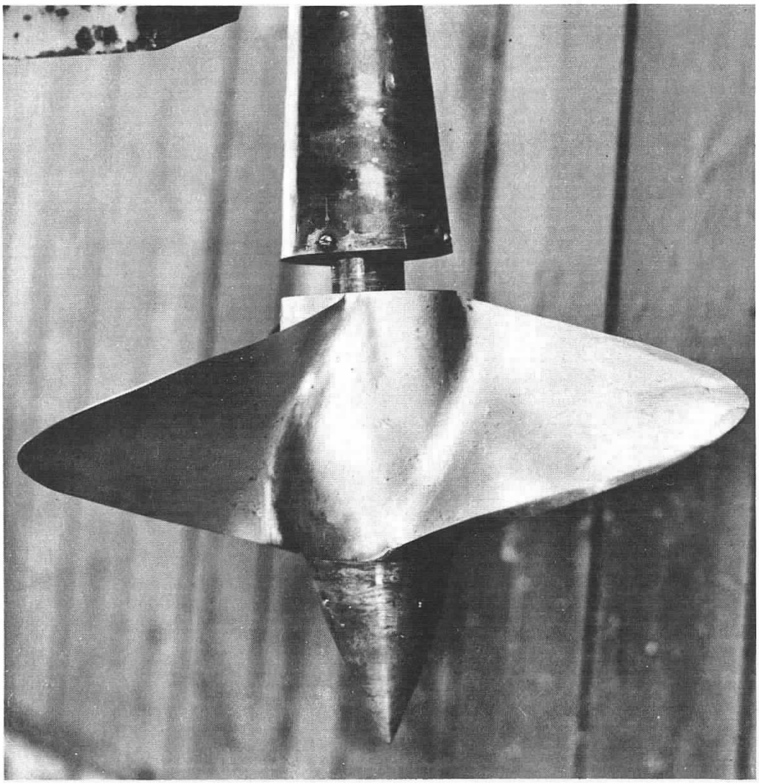

Fig. D7 - Propeller of new DTMB series, mounted on craft

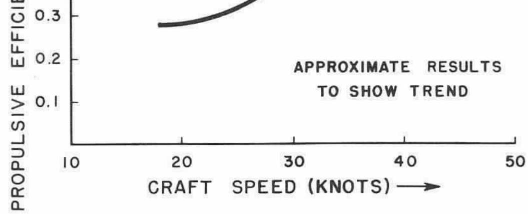

Fig. D8 - Plot of propulsive efficiency
vs craft speed (knots)

D. C. O'Neill (British Admiralty)

Our thanks are due to the authors for their informative and interesting papers. The propeller designer has been concerned with the elimination of cavitation for many years. The effects of cavitation on propeller efficiency, vibration, erosion, and noise are well known. The present papers provide a solution to the problem when such high speeds are contemplated that the existence of severe cavitation becomes inevitable.

To the Naval Architect, perhaps the most directly informative feature of the Tachmindji-Morgan paper is Fig. 1 which indicates the region where the supercavitating design of propeller is likely to be applicable. Inspection of this diagram shows that very high speeds of advance are required. For example, at $J = 0.6$ the corresponding speed for a practical SC propeller is of the order of 40-50 knots. At higher values of J this minimum speed rises to 70-80 knots. In each case, high shaft speeds and small propeller diameters are appropriate. To attain the high ship speeds in other than very small, fast craft, a significant increase in the power-to-weight ratio of existing machinery would be required. In this connection, the high shaft speed and the possibility of dispensing with reduction gearing is attractive.

To refer to points of detail, the authors have stressed their requirement for a blade section shape having a very thin leading edge in order to form the optimum cavity shape. In uniform flow this condition may well be obtained, but in the inclined and nonuniform flow behind the hull of a ship, it appears likely that fluctuations of the cavity shape will occur, leading to a reduction of efficiency and an increase in vibration and noise. The model test results shown in the paper are somewhat disappointing as the propeller, although designed for 50 knots speed of advance and running at 3000 rpm, falls within the marginal zone in Fig. 1. This serves, indeed, to emphasize the limitation of application of SC propellers referred to previously. In this marginal zone the propeller characteristics behave similar to those of more conventional propellers designed to reduce cavitation. This applies even at a cavitation number of 0.3 where one might expect the "marginal" SC design to show an advantage due to the decline of the conventional propeller's performance with increasing cavitation.

Further test results of model propellers designed and operated well within the supercavitating region will provide a more informative comparison with conventional "reduced cavitation" designs. It is hoped that the authors will extend their valuable researches to include tests of the propellers over a range of shaft inclinations and to investigate the effects of nonuniform flow.

J. P. Breslin (Stevens Institute of Technology)

The favorable prospects as outlined by Professor Lerbs should have a two-fold effect on naval engineers:

1. stimulate interest in the application of supercavitating propellers to high-speed ships,

2. provide them with the range of values of the controlling parameters to which any design must conform in order to obtain attractive efficiencies.

In this regard, it is to be noted that in order to achieve high efficiency it is necessary to design for moderate values of the thrust-loading coefficient as in the case of noncavitating propellers.

It would also be most instructive to have a design chart which would indicate how the hydrodynamic efficiencies of both noncavitating and supercavitating propellers are confined or limited by the restraints imposed by structural requirements. Such a chart would clearly show the importance of structural limitations and might thereby increase research on this subject.

One favorable prospect for supercavitating propellers which has not been mentioned lies in the action of such propellers in producing vibration-exciting effects. In view of the fact that a supercavitating section has a lift-slope of one-quarter of that for a fully wetted section, one might expect that the vibratory thrust developed by an SC propeller operating in a circumferentially variable wake would be something of the order of one-quarter of that produced by the noncavitating propeller in the same wake. In addition, heuristically one may at first expect that the strength of the fluctuating pressure field would also be mitigated by the presence of the elongated cavity at constant pressure; however, recent work on the field about noncavitating propellers has indicated that the "thickness effect" of the blades is not at all negligible, so it may be that a blade with a cavity will produce a large pressure pulse by virtue of its enlarged "displacement." This field can and should be computed to check the truth of such a guess. It would certainly be an important asset of SC propellers if it could be demonstrated that in addition to providing high efficiencies they also provide a large reduction in excitation of ship vibration.

Another aspect in regard to vibration lies in the fact that the applied frequencies will be considerably higher than now obtained because of the higher rpm. This may well be of significance although it may turn out that components which are not at present excited may be found to be at a resonant condition at supercavitating propeller blade frequencies.

H. E. Saunders (Capt., U.S.N., Ret.)

I would like to point out that perhaps the low efficiency, which is found with even some of the modern supercavitating propellers, is not necessarily a drawback to their use or further development. With the old, racing motorboats which used supercavitating propellers, starting thirty years ago, speeds of 100 miles per hour were reached despite propulsive efficiencies of only about 0.25. The supercavitating propellers did the job despite this low efficiency, and perhaps in many present and future applications, efficiency may not be the prime consideration.

There is another point which I would like to emphasize. It was shown and explained to some extent by Mr. Eames, in connection with the Canadian hydrofoil boat, that a standard density of the water is assumed in the inflow jet to the supercavitating propellers. However, all of us, who have looked through windows of our naval vessels and have seen the so-called water in which the propeller works, realize that the inflow jet with its air bubbles looked like a howling blizzard of snow on the western plains; one can hardly see the propeller for the entrained air. Also in recent years, we have found with our large, fast ships, for some reason not adequately explained, that greater and greater quantities of air are encountered in the inflow jet. Mr. Eames pointed out that he had cavitation behind one of the hydrofoils. He also had separation behind that sloping shaft. The upper blades on his propeller were certainly not working in green water.

Some of the air in the inflow jet comes down under the bow of the ship. Some of it is pulled out of solution due to low pressures along the ship's length. But just where all of the air comes from, we do not know. There are indications that on some of our latest and fastest ships we have pockets of air in the inflow jet which are longer than the pitch of the propellers. Thus, these are not bubbles any more but really big holes. My feeling is that while we should continue our work on the supercavitating propellers, we should also try to find out what to do about more air in the inflow jet as we get to higher speeds and perhaps even longer ships.

F. S. Burt (Admiralty Research Laboratory)

Mr. Tachmindji referred in his paper to the use of high speed computers for predicting propeller characteristics for a propeller series. We are very interested in this and would like to know if the DTMB has actually programmed a complete propeller design for computation on their computer. This is quite a formidable task as propeller design involves the use of correction factors such as Goldstein's k-factor and a correction for the lifting surface effect, which in themselves require some effort in programming. It may be of interest for you to know that at ARL we are at the moment having Ginzel camber correction factors, for the lifting surface effect, programmed for our Pegasus computer.

Incidentally, we would take slight issue with DTMB when they seem to use Lerb's angle-of-attack correction factor in addition to the Ginzel correction. We would argue that these conditions are equivalent and not complementary.

The possible disadvantage with supercavitating propellers may be in poor performance at off-design conditions. What information is there available on the performance at low speeds and at the incipient cavitation stage when the efficiency may be rather less than at the ultimate, fully cavitating state?

F. H. Todd (National Physical Laboratory, England)

My first contact with the problem of supercavitating propellers was in 1939 when an ordinary marine propeller was run up to supercavitating conditions in the propeller water tunnel at the National Physical Laboratory, Teddington. I presented the results of these experiments in a discussion on a paper given to the Institution of Naval Architects in 1944 by V. L. Posdunine, of the Moscow Academy, who developed a theoretical model of the flow picture and deduced expressions for the thrust and ideal efficiency.* It is of interest to note that he spoke at this time of "wedge-shaped blades," and although he did not give any particulars of the shapes he had in mind it would seem likely that they resembled in general those used in the present propellers.

In these early NPL experiments the efficiency at the point where supercavitation was just fully developed was some 49 percent, as compared with 61 percent at the same slip in the noncavitating condition. At still higher slips the efficiency continued to fall. This work was not continued because of the outbreak of war, but the results indicated what could be achieved by running a normal marine propeller under such conditions.

The theoretical analysis carried out by Mr. Tulin, and first presented at a Symposium in England in 1955, has shown how, by using specially designed supercavitating

*V. L. Posdunine, "On the Working of Supercavitating Propellers," paper presented to the Institution of Naval Architects, 1944.

sections, it is possible to regain a great deal of the loss in efficiency and so to produce propellers which, in supercavitating conditions, are not greatly inferior in efficiency to the corresponding ordinary marine propeller in the noncavitating condition.*

In this paper Mr. Tachmindji and Mr. Morgan have applied the pioneer work of Tulin to the actual design problem for supercavitating propellers. By adapting the standard propeller design methods developed at the David Taylor Model Basin to this new problem, they have been able to calculate, on a high-speed computer, the performance of a large number of propellers and so produce the design charts given in their paper. The calculated performance characteristics have been checked by a limited number of experiments, which have shown that the charts can be relied upon for the design of supercavitating propellers within the region covered by the series. The authors are to be congratulated on making this approach to the problem, which has enabled them to produce design charts very much more quickly and cheaply than would have been possible if all the 30 propellers had had to be made and tested in the tank. Their work will be of great interest to all propeller designers who are involved in the particular field in which such supercavitating propellers may be of value.

In this respect the authors devote considerable attention to the question of when it is desirable and possible to use this type of propeller. It is interesting to study the charts which they give to see just what the practical speeds are in representative cases so that we may gain a clearer idea of the possible fields of usefulness. In order to do this, I have worked out three examples - for a fast liner (Table 1), a destroyer (Table 2), and a high-speed motorboat (Table 3).

For the liner a draft of 32 feet has been assumed, a maximum propeller diameter of 20 feet, with 7 feet of cover above the tips and an atmospheric pressure equivalent to 33 feet of water, giving a total head, H, of 50 feet. Taking the points marked A, B, C, D and E on Fig. D9, Table 1 can be constructed. The points A and B mark the limiting time for the use of such propellers, and we see that even in this case the speeds are high - ranging from 40 to 85 knots. Perhaps the most interesting case is that at point A, where the speed is not too far beyond those at present in use or contemplated for Atlantic liners.

Assuming a total shaft horsepower of 250,000, estimates can be made, from the charts given in the paper, of the efficiency and pitch ratio, and the optimum values are also given in Table 1.

For conventional propellers, the quadruple screw arrangement using propellers of 18.6 feet diameter and 1.23 pitch ratio, running at 200 rpm, might be expected to give an efficiency of the order of 0.68, assuming no cavitation. This latter qualification is, of course, the crux of the

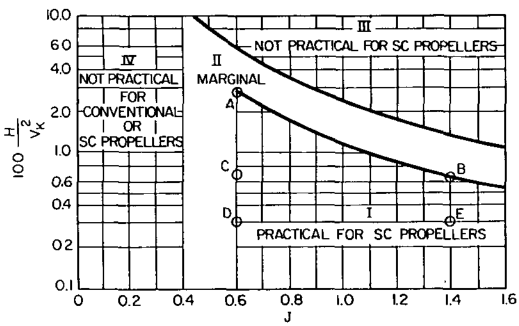

Fig. D9 - Chart of practical application of supercavitating propellers

*M. P. Tulin, "Supercavitating Flow Past Foils and Struts," Symposium on Cavitation in Hydrodynamics, NPL, 1955.

Table 1

High Speed Liner
Draft 32 feet, propeller diameter 20 feet, H = 50 feet

Point:	A			B			C			D			E		
$100\ H/V_k^2$	3.0			0.7			0.7			0.3			0.3		
V_k (knots)	40.8			84.5			84.5			129.0			129.0		
J	0.6			1.4			0.6			0.6			1.4		
Diam. (feet)	20	15	10	20	15	10	20	15	10	20	15	10	20	15	10
rpm	344	458	688	305	407	610	713	950	1426	1090	1450	2180	467	623	935

No. of screws*	4	2	4
Propeller type	Supercavitating		Conventional (assuming no cavitation)
Diam. (feet)	10	15	18.6
rpm	688	407	200
Pitch ratio	0.96	0.92	1.23
Efficiency	0.61	0.625	0.68

*Shaft horsepower: 250,000

business. In present liners of this class, cavitation is already a problem and some already suffer from cavitation erosion. To design conventional propellers to run at 40 knots or above and absorb 60,000 to 70,000 horsepower each without suffering from cavitation would therefore be a real problem, and the supercavitating propeller may well be the answer to it. Under such conditions the conventional propeller would lose some of its margin of efficiency and any remaining difference in this respect would have to be set against the absence of erosion. If we consider still faster speeds, moving along the line from A to B, the problem of designing a conventional propeller becomes rapidly more difficult and the use of supercavitating propellers more attractive.

For the destroyer and high-speed motorboat, Tables 2 and 3 can be prepared. In these two types of ship, it will be seen that even at the present top speeds the supercavitating propeller may already be considered as a rival of the conventional propeller, and it is in the high-speed motorboats that it has already been adopted on numerous occasions, although without the benefit of the new type sections.

In the past, the supercavitating propellers used have in general had normal sections of the aerofoil or crescent (hollow-faced) type, and the relatively low efficiencies of these propellers under such conditions of operation have been accepted as part of the necessary price of working in this area. It has now been shown how, with the proper choice of sections, this loss of efficiency can be avoided to a large

Table 2

Destroyer

Draft 12 feet, propeller diameter 12 feet, cover 6 feet, H = 45 feet

Point:	A			B		C		D		E	
$100\ H/V_k^2$	3.0			0.7		0.7		0.3		0.3	
V_k (knots)	38.7			80.2		80.2		122.5		122.5	
J	0.6			1.4		0.6		0.6		1.4	
Diam. (feet)	12	6	10	12	6	12	6	12	6	12	6
rpm	545	1090	655	483	966	1127	2254	1728	3456	740	1480
No. of screws*	2							2			
Propeller type†	Supercavitating							Conventional (assuming no cavitation)			
Diam. (feet)	10							12.6			
rpm	655							350			
Pitch ratio	0.94							1.18			
Efficiency	0.62							0.66			

*Shaft horsepower: 100,000
†Comparison at 38.7 knots

extent, and supercavitating propellers can be designed to give reasonable efficiencies under very advanced design conditions, thus extending the range over which marine propellers may continue to be used for high-speed ship propulsion.

An inspection of the tables will also show the wide range of revolutions possible with such propellers, and this feature may well be of great interest to the marine engineer, enabling him to consider the adoption of lighter, faster-running engines and the elimination of gearing.

Of course, as in most new developments, the supercavitating propeller also brings its own problems, and one of the most important of these will undoubtedly be the need to obtain sufficient strength in the blades, particularly near the very fine leading edge. To avoid distortion and vibration in this vicinity will call for extremely hard and tough material.

Also, it is important to realize the limitations of this type of propeller. Many new ideas have been spoiled in the past because attempts were made to apply them indiscriminately in fields where their particular merits could not be realized. From the examples quoted above, it will be realized that the essential condition for the use of the supercavitating propeller is a relatively high speed. It will not assist the normal cargo ship to go faster, but in the field of high-speed motorboats and destroyers it may be considered as a practical propeller even with present-day speeds.

Table 3

High Speed Motorboat
Immersion to centreline shaft assumed 7 feet, H = 40 feet

Point:	A			B		C		D		E	
100 H/V_k^2	3.0			0.7		0.7		0.3		0.3	
V_k (knots)	36.5			75.5		75.5		115.5		115.5	
J	0.6			1.4		0.6		0.6		1.4	
Diam. (feet)	4	3	2	4	2	4	2	4	2	4	2
rpm	1540	2055	3080	1363	2726	3185	6370	4875	9750	2090	4180

No. of screws*	4	4
Propeller type†	Supercavitating	Conventional (assuming no cavitation)
Diam. (feet)	2.40	2.38
rpm	2570	1800
Pitch ratio	0.90	1.16
Efficiency	0.64	0.67

*Shaft horsepower: 8000
†Comparison at 36.5 knots

It is, indeed, interesting to note that its field of useful application begins just about at the point which we have now reached in such high-speed craft and even in Atlantic liners, and if the demand for still higher speeds in these classes of ships continues, then the supercavitatingpropeller has a promisingfield in front of itand the designer a useful new weapon in his armoury.

A. Silverleaf (National Physical Laboratory)

These papers summarize a very great amount of work, and the information which they give is an immense aid to those of us who do not yet have any personal experience with supercavitating propellers. My first reaction to the paper by Mr. Tachmindji and Mr. Morgan is surprise in that design methods developed for orthodox propellers (in the development of which Prof. Lerbs has played a major role) appear to work so well for supercavitating conditions. Do the physical conditions in the wake immediately downstream of a screw with long cavities over the backs of its blades closely resemble those postulated for the conventional vortex-theory design method for propellers? Prof. Lerb's review of the flow models for supercavitating propellers suggests to me that a more complicated model may be necessary to understand fully the action of supercavitating propellers.

The pitch correction factors presented by Mr. Tachmindji and Mr. Morgan are clearly derived from a very extensive analysis, but I find them difficult to understand. Does the correction for finite cavitation number take account of the very marked radial variation in the local cavitation number, which in most propellers covers a range of about 8 to 1? Further, can Ludwigg-Ginzel curvature correction factors, which depend closely on the blade width, apply to supercavitating propellers? What is the effective chord of a blade which has a long cavity extending far downstream of its trailing edge?

The principle of carrying out systematic design calculations before indulging in the costly, time-consuming, and often disappointing process of systematic model experiments is an excellent one, and undoubtedly Mr. Tachmindji and Mr. Morgan have applied it most thoroughly. However, I am not entirely clear how the curves of his Figs. 6 and 7 are computed; has the inverse of a design method been developed to calculate the performance characteristics of propellers with specified geometry, or has the design method itself been directly applied to determine the geometrical features of propellers satisfying a set of specified operating conditions? If the latter method has been followed, then presumably each of the thirty propellers for which calculations were made is an optimum design, and thus each curve of constant pitch ratio in Figs. 6 and 7 embraces a set of propellers which are otherwise not geometrically identical, unlike similar diagrams for conventional propeller series.

Mr. Tachmindji and Mr. Morgan claim satisfactory agreement between measured performance values for a number of supercavitating propellers and those derived from the calculated series. How were the experimental values determined? If they were based on water-tunnel test data, then what tunnel interference correction factors were used? It seems unlikely that simple corrections are adequate.

There is a brief reference to the possibility of using forced ventilation to operate supercavitating propellers at low ship and shaft rotation speeds. How much power would be needed to operate the necessary ancillary gear? Experiments with model supercavitating screws in a towing tank should help to answer such questions. What is the efficiency of supercavitating propellers when rotating in the astern direction? If it is low, then I should expect supercavitating propellers to be used for ships with shafts rotating unidirectionally; if so, then controllable pitch screws would be necessary. How do supercavitating sections behave over a wide range of pitch settings? Finally, it is important to remember that very large thrusts are needed to propel large ships; practical considerations of propeller blade strength may well be decisive factors in the ultimate adoption of supercavitating propellers for large, fast ships.

H. Lerbs

One question to which I would like to reply immediately was that by Mr. Burt. The question refers to the lifting surface effects of the propeller and the corrections which are necessary when you take the section property from two-dimensional flow.

Now, the lifting surface effect exhibits itself in the curvature of the streamlines, and if the lifting surface effect of the propeller were such that the curvature over the chord length would be constant, Ludwig's correction would suffice. Now, owing to the continuous change of the velocity the curvature of the flow is smaller at the leading edge and greater at the trailing edge, and in order to compensate for this change of curvature an angle of attack is necessary.

A. J. Tachmindji

I'd like to reply briefly to a few points. Regarding Mr. Rader's comments on the question of speed, I think he has misunderstood the 50 knot question. The important thing, of course, is cavitation number and not speed. The value of speed itself is immaterial.

Mr. O'Neill told us on the one hand that the supercavitating propeller was not quite comparable to the ones at AEW and then he showed us very nicely that this was in the marginal region. This was the basic reason that the diagram of Fig. 1, was given, i.e., to anticipate the comparison with arbitrary propellers. Of course, it has been shown that the efficiency of conventional propellers drops quite rapidly at low cavitation numbers.

On Mr. Burt's comments about computing machines, we do have at the Model Basin a complete program for computing machines. The method used there is induction factor method rather than the Goldstein method. It's a bit easier to program this particular method.

Dr. Todd has pointed out the ranges and speeds of supercavitating propellers.

Mr. Silverleaf has given a glimmer of some of the work necessary to produce this diagram and he is quite right in saying there is more to it than meets the eye.

Regarding the estimated performance of propellers in water tunnels, the one which was given was tested in full scale and also tested in the Basin and most of the work which has been carried on in the water tunnels is duplicated in the Basin.

* * * * *